General Framework and Algorithm for Data Rate Maximization in DSL Networks

Rodrigo B. Moraes, *Member, IEEE*, Paschalis Tsiaflakis, *Member, IEEE*, Jochen Maes, *Senior Member, IEEE*, and Marc Moonen, *Fellow, IEEE*

***Abstract*— In this paper, we treat the combined signal and spectrum coordination problem in digital subscriber line (DSL) networks with linear design for transmitters and receivers. The transmission is modeled as a multitone MIMO system where each user has a number of transceivers and there is coordination between sets of users on the transmitter and on the receiver sides. We consider the possibility of an asynchronous transmission, i.e. when the transmission of DMT blocks for different users is not aligned in time. This gives rise to inter-carrier interference. Our objective is the maximization of the weighted sum of users' data rates subject to power constraints. Although this problem is well known in the literature, previous works have always based their designs on strong assumptions about the network infrastructure. In this paper, we propose a general framework and algorithm that apply for any infrastructure, including any number of users, any number of transceivers, any number of tones, any kind of coordination on both the transmitter and on the receiver sides, and synchronous or asynchronous transmission. We also do not assume any special structure of the channel matrix. Our algorithm is seen to perform very well and is polynomial time solvable.**

***Index Terms*—DSL, crosstalk, optimization, MIMO.**

I. Introduction

MULTI-INPUT, multiple-output (MIMO) processing has constituted a paradigm shift in the way communication systems are designed. It has captured the attention of researchers and the telecommunication industry since the 1990's, when it was first studied. The technology is an undeniable success, and within a decade it has evolved from a theoretical concept to practical implementation [1].

The initial research efforts in MIMO communications were focused mainly on single-user systems, but the focus quickly evolved to multi-user scenarios [2]. In these scenarios, the extra spatial dimensions serve the purpose of spatial separation of the different users, providing the means for interference mitigation and thus an improved channel utilization. Multi-user MIMO is classically divided into three situations, depending on how much coordination there is on the receiver and on the transmitter sides. A system with full transmitter coordination is called a broadcast channel (BC), whereas a system with full receiver coordination is called a multiple access channel (MAC). When there is no inter-user coordination neither on the transmitter nor on the receiver side, the scenario is referred to as an interference channel (IC).

Most of the research and standardization activities when it comes to MIMO technology have focused on wireless transmission. However, the same paradigm can be applied to any multi-transceiver scenario where there are cross channel gains between all transmitters and all receivers.[1] A digital subscriber line (DSL) binder fits such a description. In DSL, multiple users transmit over closely packed copper pairs. Because of electromagnetic radiation, a signal transmitted in a given pair leaks to the neighboring pairs. This phenomenon is known as crosstalk. Crosstalk has been traditionally identified as the main source of performance degradation for such systems, but, with MIMO processing, crosstalk can be used as a means to improve performance. After all, crosstalk contains signal energy that can be detected on the other side of the network [3]. It is the processing of the signals that defines whether crosstalk is beneficial or detrimental to performance.

By far the world's favorite means of broadband access, DSL counts more than 400 million subscribers and a market share of more than 70% [4]. Although it is predicted that DSL will eventually be replaced with optical fiber even for home use, it is expected that DSL will be around as an important market technology for decades.

To expand its lifetime as much as possible and to keep competitive, DSL technology has been evolving in two main directions. First, as a result of the expansion of the optical

Manuscript received July 4, 2013; revised November 27, 2013 and January 29, 2014. The editor coordinating the review of this paper and approving it for publication was S. Galli.

This research work was carried out at the ESAT Laboratory of the KU Leuven, in the framework of the KU Leuven Research Council PFV/10/002 (OPTEC); the Bilateral Scientific Cooperation between Tsinghua University & KU Leuven 2012-2014; the FWO project G091213N 'Cross-layer optimization with real-time adaptive dynamic spectrum management for fourth generation broadband access networks'; the Belgian Programme on Interuniversity Attraction Poles initiated by the Belgian Federal Science Policy Office, 'Belgian network on Stochastic modeling, analysis, design and optimization of communication systems' (BESTCOM) 2012-2017; and the Concerted Research Action GOA-MaNet. The scientific responsibility is assumed by the authors.

R. B. Moraes and P. Tsiaflakis were with the STADIUS Center for Dynamical Systems, Signal Processing and Data Analytics, Department of Electrical Engineering (ESAT), KU Leuven, Kasteelpark Arenberg 10, B-3001 Leuven, Belgium. They are now with Access Research Domain, Alcatel-Lucent Bell Labs, Antwerp, Belgium (e-mail: rodrigo.moraes@alcatel-lucent.com, paschalis.tsiaflakis@alcatel-lucent.com).

J. Maes is with the Access Research Domain, Alcatel-Lucent Bell Labs, Antwerp, Belgium (e-mail: jochen.maes@alcatel-lucent.com).

M. Moonen is with the STADIUS Center for Dynamical Systems, Signal Processing and Data Analytics, Department of Electrical Engineering (ESAT), KU Leuven, Kasteelpark Arenberg 10, B-3001 Leuven, Belgium (e-mail: marc.moonen@esat.kuleuven.be).

Digital Object Identifier 10.1109/TCOMM.2014.030214.130507

[1] We define a transceiver as a generalization of the concept of DSL line. A transceiver is connected to a physical channel that can be a direct mode or common mode of a copper pair or the phantom mode of two copper pairs or one wire in split wire signaling. In wireless parlance, 'antenna' is a similar concept.

0090-6778/14$31.00 © 2014 IEEE

fiber network, copper lines are getting shorter. In the future, it is foreseen that DSL will be responsible for bridging the last couple of hundred meters from the fiber-fed last distribution point to the customer premisses equipment (CPE). Accordingly, standardization bodies have been working on new types of DSL better suited for shorter lines. E.g. future generations standards include the G.fast, which will go into the market around 2016 and is designed to work on copper lines that are at most a couple of hundred meters long. The second direction of evolution results from the decade-long research activities that aim at amplifying DSL's advantages from a signal processing perspective. This body of work is called dynamic spectrum management (DSM) and its main goal is to deal with crosstalk interference—in the DSL context, DSM that involves MIMO processing is often called *vectoring* or DSM level 3 [5]. We remark that MIMO processing in DSL also encompasses the possibility of the utilization of common mode (CM), phantom mode (PM) or split wire (SW) transmission [3], [6]. While the first direction of evolution is about the physical infrastructure of the access network (i.e. bringing the network hardware closer to the CPE), DSM techniques rely on intelligent coordination and processing of signals (i.e. expanding the functionality of the network software). It has been repeatedly shown in the literature that applying DSM leads to formidable gains.

Given a DSL network, depending on the kind of coordination on the transmitter and on the receiver sides, e.g. receiver-only, transmitter-only, etc., a BC, a MAC, an IC or a combination of them can be used as a model. Several papers have focused on the design of the transmission and reception strategies for such scenarios, e.g. [5], [7]–[15]. However, it is observed that these references base their designs on strong assumptions about the network infrastructure. We give four examples of these assumptions.

- First, most previous work considers a synchronous transmission case, i.e. the situation when all users' discrete multitone (DMT) blocks are aligned (i.e. time synchronized) at the receivers. This is not necessarily the case. Users who are in different physical locations or who belong to different service providers are difficult to synchronize. The result of asynchronous DMT transmission is inter-carrier interference (ICI) [16]–[19], which complicates the problem significantly.
- Some previous references [5], [7], [8], [12] assume that in DSL coordination is only possible on the central office (CO) side of the network.[2] In other words, there is either a BC scenario for downstream transmission or a MAC scenario for upstream transmission. We believe this is too restrictive. E.g. it can be that a number of DSL lines arrive at the same box on the CPE if the connection serves a large residential building. This allows for some limited coordination on the CPE side as well. Plus, if two copper pairs that arrive on the CPE use PM transmission, then there is a three transceiver system that can be coordinated on the CPE side.
- Another assumption is that every user uses only one line (or one transceiver). This is not always the case. There are places where it is not uncommon that there are two DSL lines connected to a user. In some places, quads are popular. A quad is a group of four copper wires twisted together that serve a single customer. In these cases, pair bonding, CM, PM or SW transmission can then be used.
- A final common assumption is that DSL channels have the so-called property of column-wise or row-wise diagonal dominance [7], [8], [12]. However, this only holds true for the case when sources of noise other than crosstalk are spatially white.

We believe there is a much richer range of interesting scenarios than what hitherto has been considered. Telephone networks have evolved differently through the decades in different parts of the world, giving rise to complex networks that have each their characteristics. Many of these networks would probably not fit on the scenarios considered previously in the literature. Modern DSL networks are likely better represented by an abundant set of different hybrid scenarios, where users can have multiple transceivers and elements of IC, MAC and BC are present. In this work we consider a general scenario that encompasses all these hybrid situations as special cases.

To the best of our knowledge, no work up to now has developed a general framework and a corresponding algorithm that apply to this general scenario. This is the goal of this paper. We develop a general system framework that includes MAC, BC and IC and any combination of them as a special case (we consider only linear transmission schemes). We propose an algorithm similar to the one in [20] that works for all cases, including any number of users, any number of transceivers, any number of tones, any kind of coordination on both the transmitter and on the receiver sides, and synchronous or asynchronous transmission. Through numerical simulations, the algorithm is seen to perform very well and is shown to be polynomial time solvable.

We organize this paper as follows. Section II presents the system model, the notation, the problem of interest and previous solutions. In Section III we derive and present our proposed approach. Section IV contains some simulation results and Section V presents final remarks.

We use lower-case boldface letters to denote vectors, upper-case boldface letters for matrices and calligraphic letters for sets (e.g. $\mathbf{a}$, $\mathbf{A}$ and $\mathcal{A}$). We use $\mathbf{I}_A$ as the identity matrix of size A, $\mathbf{0}_{A\times B}$ as the $A \times B$ matrix of zeros, $\mathbb{R}_+$ as the set of non-negative real numbers, $(\cdot)^{\mathrm{T}}$ as the transpose, $(\cdot)^{\mathrm{H}}$ as the Hermitian transpose, $(\cdot)^*$ as the complex conjugate, $\mathrm{E}[\cdot]$ as expectation, $\mathrm{tr}\{\cdot\}$ as trace, $|\cdot|$ as determinant and $\mathrm{diag}\{\mathbf{a}\}$ as the matrix with a vector $\mathbf{a}$ on the main diagonal.

II. System Model and Problem Statement

A. System model and notation—Synchronous case

This is the only section in this paper where we specifically treat the *synchronous* transmission situation. That is so because the aim of this section is to present the notation we use and to see the effects of adding coordination on the transmitter and receiver sides of the network. To consider the asynchronous

[2]By 'coordination on the CO side of the network' we mean that coordination can be done on the CO itself, in a fiber-fed cabinet in the street, a distribution point or in the basement of a large building.

situation here would be too cumbersome. All conclusions from this section are readily extendable to the more general asynchronous case.

We consider an N user DSL system with DMT modulation with K Δ_f-spaced tones. We consider a system where upstream and downstream transmission are separated (with, e.g. time or frequency division duplexing), hence the crosstalk we consider is far end crosstalk (FEXT).[3] We denote the set of users by $\mathcal{N} = \{1, \ldots, N\}$ and the set of tones by $\mathcal{K} = \{1, \ldots, K\}$. We let p_n^k be the transmit power of user n on tone k and we organize these values in the matrix $\mathbf{P} \in \mathbb{R}_+^{K \times N}$. The nth column of $\mathbf{P}$, denoted by $\mathbf{p}_n = \begin{bmatrix} p_n^1 & \ldots & p_n^K \end{bmatrix}^{\mathrm{T}} \in \mathbb{R}_+^K$, contains the power allocation of user n in all tones. The kth row of $\mathbf{P}$, $\mathbf{p}^k = \begin{bmatrix} p_1^k & \ldots & p_N^k \end{bmatrix} \in \mathbb{R}_+^N$, represents the power allocation of all users in tone k. User n has A_n transceivers.

Every user belongs to a group both on the transmitter side and on the receiver side. Inside a group, users can apply coordinated MIMO processing. We define each group as a set. For the grouping on the transmitter side, we define $\mathcal{G}_i^{\mathrm{tx}}$, $i = 1, \ldots, I \leq N$. For the grouping on the receiver side, we similarly define $\mathcal{G}_q^{\mathrm{rx}}$, $q = 1, \ldots, Q \leq N$. Here I and Q denote the number of groups on the transmitter and on the receiver sides, respectively. A user can only be in a single group both on the transmitter and on the receiver sides, i.e. if $n \in \mathcal{G}_i^{\mathrm{tx}}$ then $n \notin \mathcal{G}_q^{\mathrm{tx}},\ q \neq i$ and if $n \in \mathcal{G}_q^{\mathrm{rx}}$ then $n \notin \mathcal{G}_i^{\mathrm{rx}},\ q \neq i$. We also define the number of transceivers per group on the transmitter and on the receiver sides respectively as

$$A_{\mathcal{G}_i^{\mathrm{tx}}} = \sum_{n \in \mathcal{G}_i^{\mathrm{tx}}} A_n \tag{1}$$

$$A_{\mathcal{G}_q^{\mathrm{rx}}} = \sum_{n \in \mathcal{G}_q^{\mathrm{rx}}} A_n \tag{2}$$

As already mentioned, throughout this paper we focus on a linear design for both transmitters and receivers and treat interference as noise. All channel gains are considered perfectly known. Taking this into account, we obtain the received signal vector for group $\mathcal{G}_q^{\mathrm{rx}}$ on tone k and the estimated signal vector for user n on tone k respectively as

$$\mathbf{y}_{\mathcal{G}_q^{\mathrm{rx}}}^k = \underset{n \in \mathcal{G}_q^{\mathrm{rx}}}{\mathrm{vec}} [\mathbf{y}_n^k] \tag{3}$$

$$\hat{\mathbf{x}}_n^k = \mathbf{R}_n^k \mathbf{y}_{\mathcal{G}_q^{\mathrm{rx}}}^k,\ n \in \mathcal{G}_q^{\mathrm{rx}} \tag{4}$$

Here $\mathbf{y}_{\mathcal{G}_q^{\mathrm{rx}}}^k \in \mathbb{C}^{A_{\mathcal{G}_q^{\mathrm{rx}}}}$ is a concatenation of the received signal vectors $\mathbf{y}_n^k \in \mathbb{C}^{A_n}$ of the users that belong to $\mathcal{G}_q^{\mathrm{rx}}$. For example, if $\mathcal{G}_q^{\mathrm{rx}} = \{1, 2, 3\}$, then $\mathbf{y}_{\mathcal{G}_q^{\mathrm{rx}}}^k = [(\mathbf{y}_1^k)^{\mathrm{T}} \ (\mathbf{y}_2^k)^{\mathrm{T}} \ (\mathbf{y}_3^k)^{\mathrm{T}}]^{\mathrm{T}}$. In (4), we have $\hat{\mathbf{x}}_n^k \in \mathbb{C}^{A_n}$. Eqs. (3) and (4) are specified in detail later with some examples. For now, we just mention that they depend on five variables:

- $\mathbf{x}_n^k \in \mathbb{C}^{A_n}$, the transmitted signal vector for user n on tone k.
- $\mathbf{T}_n^k \in \mathbb{C}^{A_{\mathcal{G}_i^{\mathrm{tx}}} \times A_n}$, the transmit matrix for user n on tone k, where $n \in \mathcal{G}_i^{\mathrm{tx}}$.
- $\mathbf{R}_n^k \in \mathbb{C}^{A_n \times A_{\mathcal{G}_q^{\mathrm{rx}}}}$, the receive matrix for user n on tone k, where $n \in \mathcal{G}_q^{\mathrm{rx}}$.
- $\widetilde{\mathbf{H}}_{n,j}^k$, $n, j \in \mathcal{N}$, the channel matrix on tone k between the transmitter of user j and the receiver of user n. The size of $\widetilde{\mathbf{H}}_{n,j}^k$ depends on the groups on both transmitter and receiver sides, i.e. $\widetilde{\mathbf{H}}_{n,j}^k \in \mathbb{C}^{A_{\mathcal{G}_{\mathrm{rx}}^q} \times A_{\mathcal{G}_{\mathrm{tx}}^i}}$, where q and i are such that $n \in \mathcal{G}_{\mathrm{rx}}^q$ and $j \in \mathcal{G}_{\mathrm{tx}}^i$.
- $\mathbf{z}_{\mathcal{G}_q^{\mathrm{rx}}}^k \in \mathbb{C}^{A_{\mathcal{G}_q^{\mathrm{rx}}}}$, a vector of circularly symmetric zero mean complex Gaussian noise. It is a concatenation of vectors similar to (3), i.e. $\mathbf{z}_{\mathcal{G}_q^{\mathrm{rx}}}^k = \mathrm{vec}_{n \in \mathcal{G}_q^{\mathrm{rx}}}[\mathbf{z}_n^k]$, where $\mathbf{z}_n^k \in \mathbb{C}^{A_n}$.

We assume that $\mathbf{x}_n^k$ has A_n parallel data streams, but some of these streams can have rate of zero. We also assume $\mathrm{E}\left[\mathbf{x}_n^k (\mathbf{x}_n^k)^{\mathrm{H}}\right] = \mathbf{I}_{A_n}$. The noise vector $\mathbf{z}_{\mathcal{G}_q^{\mathrm{rx}}}^k$ is assumed to be spatially white with covariance matrix $\mathrm{E}\left[\mathbf{z}_{\mathcal{G}_q^{\mathrm{rx}}}^k (\mathbf{z}_{\mathcal{G}_q^{\mathrm{rx}}}^k)^{\mathrm{H}}\right] = \mathbf{I}_{A_{\mathcal{G}_q^{\mathrm{rx}}}}$, $q = 1 \ldots, Q$.

We now specify (3) and (4) in three examples. The main point of these examples is to show that $\widetilde{\mathbf{H}}_{n,j}^k$ depends on the type of coordination on both sides of the channel and that it can be viewed as a concatenation of matrices relating to the MIMO IC, that we define as $\mathbf{H}_{n,j}^k \in \mathbb{C}^{A_n \times A_j}\ \forall n, j$.

The **first example** is depicted in Fig. 1. This is a system with three users and three tones. This is a pure MIMO IC, i.e. every group contains a single user. This is the situation where there is a minimum amount of coordination. We have $Q = I = N = 3$ and $\mathcal{G}_n^{\mathrm{tx}} = \mathcal{G}_n^{\mathrm{rx}} = \{n\}$, $n \in \mathcal{N}$. In this case, we write

$$\mathbf{y}_{\mathcal{G}_n^{\mathrm{rx}}}^k = \mathbf{y}_n^k = \sum_{j \in \mathcal{N}} \mathbf{H}_{n,j} \mathbf{T}_j^k \mathbf{x}_j^k + \mathbf{z}_n^k \tag{5}$$

$$\hat{\mathbf{x}}_n^k = \mathbf{R}_n^k \underbrace{\mathbf{H}_{n,n}^k}_{\triangleq \widetilde{\mathbf{H}}_{n,n}^k} \mathbf{T}_n^k \mathbf{x}_n^k + \sum_{j \neq n} \mathbf{R}_n^k \underbrace{\mathbf{H}_{n,j}^k}_{\triangleq \widetilde{\mathbf{H}}_{n,j}^k} \mathbf{T}_j^k \mathbf{x}_j^k + \mathbf{R}_n^k \mathbf{z}_n^k \tag{6}$$

We define $\widetilde{\mathbf{H}}_{n,j}^k$, $n, j \in \mathcal{N}$ as the channel matrix that comes between $\mathbf{R}_n^k$ and $\mathbf{T}_j^k$. In this first example, for all tones we have $\widetilde{\mathbf{H}}_{n,j}^k = \mathbf{H}_{n,j}^k$, $n, j \in \mathcal{N}$; $A_{\mathcal{G}_n^{\mathrm{tx}}} = A_{\mathcal{G}_n^{\mathrm{rx}}} = A_n$ and $\mathbf{T}_n^k, \mathbf{R}_n^k \in \mathbb{C}^{A_n \times A_n}$, $n \in \mathcal{N}$.

The **second example** is depicted in Fig. 2. This is a system with three users, with, say $A_1 = 2$, $A_2 = 3$ and $A_3 = 1$, and three tones. There are two groups on both transmitter and receiver sides, i.e. $Q = I = 2$. We have $\mathcal{G}_1^{\mathrm{tx}} = \{1\}$ and $\mathcal{G}_2^{\mathrm{tx}} = \{2, 3\}$; and on the receiver side $\mathcal{G}_1^{\mathrm{rx}} = \{1, 2\}$ and $\mathcal{G}_2^{\mathrm{rx}} = \{3\}$. Using (1) and (2), we obtain $A_{\mathcal{G}_1^{\mathrm{tx}}} = 2$, $A_{\mathcal{G}_2^{\mathrm{tx}}} = 4$, $A_{\mathcal{G}_1^{\mathrm{rx}}} = 5$ and $A_{\mathcal{G}_2^{\mathrm{rx}}} = 1$. As a consequence, for all tones we have $\mathbf{T}_1^k \in \mathbb{C}^{2 \times 2}$, $\mathbf{T}_2^k \in \mathbb{C}^{4 \times 3}$, etc. Notice that this system does not fit exactly neither the MAC, nor the BC, nor the IC case. This is a scenario with elements of BC, MAC and IC.

To calculate the equivalent channel matrices, we take into account the matrices $\mathbf{H}_{n,j}^k \in \mathbb{C}^{A_n \times A_j}$, $n, j \in \mathcal{N}$ and $k \in \mathcal{K}$. As mentioned in a previous paragraph, these are the channel matrices for the case of a pure MIMO IC. The received signal for, say, group 1 is given by

$$\mathbf{y}_{\mathcal{G}_1^{\mathrm{rx}}}^k = \begin{bmatrix} \mathbf{y}_1^k \\ \mathbf{y}_2^k \end{bmatrix} = \begin{bmatrix} \mathbf{H}_{1,1}^k \\ \mathbf{H}_{2,1}^k \end{bmatrix} \mathbf{T}_1^k \mathbf{x}_1^k + \begin{bmatrix} \mathbf{H}_{1,2}^k & \mathbf{H}_{1,3}^k \\ \mathbf{H}_{2,2}^k & \mathbf{H}_{2,3}^k \end{bmatrix} \mathbf{T}_2^k \mathbf{x}_2^k + \begin{bmatrix} \mathbf{H}_{1,2}^k & \mathbf{H}_{1,3}^k \\ \mathbf{H}_{2,2}^k & \mathbf{H}_{2,3}^k \end{bmatrix} \mathbf{T}_3^k \mathbf{x}_3^k + \begin{bmatrix} \mathbf{z}_1^k \\ \mathbf{z}_2^k \end{bmatrix}. \tag{7}$$

The estimated signal for, say, user 2 is given by applying (4),

[3]The system model can be straightforwardly generalized to a situation where upstream and downstream transmission are jointly optimized, eventually taking near end crosstalk (NEXT) into account.

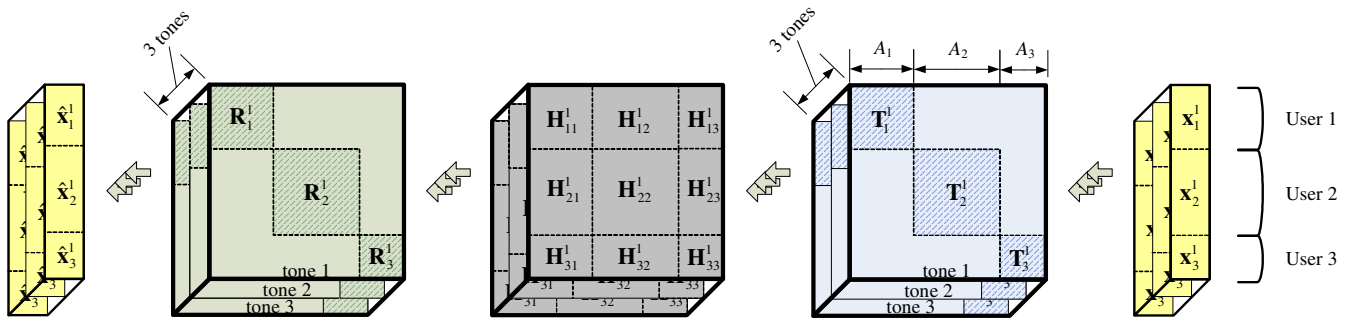

Fig. 1. Illustration of a MIMO IC. For this case, there is only one user on every group in both the transmitter and on the receiver sides. Here, we have $Q = I = N = 3$ and $\mathcal{G}_n^{\text{tx}} = \mathcal{G}_n^{\text{rx}} = \{n\}$, $n = 1, \ldots, 3$.

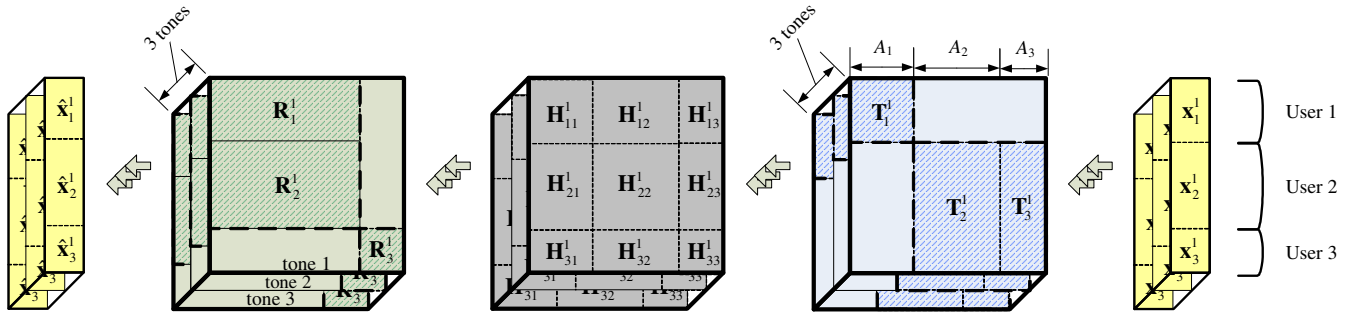

Fig. 2. Illustration of a hybrid MAC, BC and IC. For this case, we have on the transmitter side $\mathcal{G}_1^{\text{tx}} = \{1\}$ and $\mathcal{G}_2^{\text{tx}} = \{2, 3\}$; and on the receiver side $\mathcal{G}_1^{\text{rx}} = \{1, 2\}$ and $\mathcal{G}_2^{\text{rx}} = \{3\}$.

i.e.

$$\hat{\mathbf{x}}_2^k = \mathbf{R}_2^k \underbrace{\begin{bmatrix} \mathbf{H}_{1,1}^k \\ \mathbf{H}_{2,1}^k \end{bmatrix}}_{\triangleq \widetilde{\mathbf{H}}_{2,1}^k} \mathbf{T}_1^k \mathbf{x}_1^k + \mathbf{R}_2^k \underbrace{\begin{bmatrix} \mathbf{H}_{1,2}^k & \mathbf{H}_{1,3}^k \\ \mathbf{H}_{2,2}^k & \mathbf{H}_{2,3}^k \end{bmatrix}}_{\triangleq \widetilde{\mathbf{H}}_{2,2}^k} \mathbf{T}_2^k \mathbf{x}_2^k + \mathbf{R}_2^k \underbrace{\begin{bmatrix} \mathbf{H}_{1,2}^k & \mathbf{H}_{1,3}^k \\ \mathbf{H}_{2,2}^k & \mathbf{H}_{2,3}^k \end{bmatrix}}_{\triangleq \widetilde{\mathbf{H}}_{2,3}^k} \mathbf{T}_3^k \mathbf{x}_3^k + \mathbf{R}_2^k \mathbf{z}_{\mathcal{G}_1^{\text{rx}}}^k. \quad (8)$$

Again we use the definition of $\widetilde{\mathbf{H}}_{n,j}^k$, $n, j \in \mathcal{N}$, i.e it is the channel matrix that comes between $\mathbf{R}_n^k$ and $\mathbf{T}_j^k$. Here we see that with added coordination, $\widetilde{\mathbf{H}}_{n,j}^k$ becomes a concatenation of the matrices $\mathbf{H}_{n,j}^k$. The concatenation depends on the grouping on both the receiver and transmitter sides.

The **third example** is that of a three user MIMO BC. This system is represented by $\mathcal{G}^{\text{tx}} = \{1, 2, 3\}$, i.e. $I = 1$, and $\mathcal{G}_n^{\text{rx}} = \{n\}$, $n \in \mathcal{N}$, i.e. $Q = 3$. If $A_n = 2\ \forall n$, then $A_{\mathcal{G}^{\text{tx}}} = 6$ and $A_{\mathcal{G}_q^{\text{rx}}} = 2$, $s = 1, 2, 3$. For this case, we for the equivalent channel matrices as

$$\widetilde{\mathbf{H}}_{1,n}^k = \begin{bmatrix} \mathbf{H}_{1,1}^k & \mathbf{H}_{1,2}^k & \mathbf{H}_{1,3}^k \end{bmatrix}, \ n \in \mathcal{N} \quad (9)$$

$$\widetilde{\mathbf{H}}_{2,n}^k = \begin{bmatrix} \mathbf{H}_{2,1}^k & \mathbf{H}_{2,2}^k & \mathbf{H}_{2,3}^k \end{bmatrix}, \ n \in \mathcal{N} \quad (10)$$

$$\widetilde{\mathbf{H}}_{3,n}^k = \begin{bmatrix} \mathbf{H}_{3,1}^k & \mathbf{H}_{3,2}^k & \mathbf{H}_{3,3}^k \end{bmatrix}, \ n \in \mathcal{N} \quad (11)$$

After these three examples, we can now focus on the general case. We write (4) as

$$\hat{\mathbf{x}}_n^k = \mathbf{R}_n^k \widetilde{\mathbf{H}}_{n,n}^k \mathbf{T}_n^k \mathbf{x}_n^k + \mathbf{R}_n^k \sum_{j \neq n} \widetilde{\mathbf{H}}_{n,j}^k \mathbf{T}_j^k + \mathbf{R}_n^k \mathbf{z}_{\mathcal{G}_q^{\text{rx}}}^k, \ n \in \mathcal{G}_q^{\text{rx}}. \quad (12)$$

Because of the structure with groups and because the $\widetilde{\mathbf{H}}_{n,j}^k$ are defined as functions of the $\mathbf{H}_{n,j}^k$, (12) includes any kind of transmitter and receiver coordination. On one extreme, we have a MIMO IC, as explained in the first example. On the other extreme, there is only one group both on the transmitter and on the receiver side, i.e. $\mathcal{G}^{\text{tx}} = \mathcal{G}^{\text{rx}} = \{1, \ldots, N\}$. This is the case with full two-sided coordination. It is often called a MIMO point-to-point system. With our formulation, every case between (and including) these two extremes is possible.

As a rule of thumb, we remark that coordination on the transmitter side makes $\widetilde{\mathbf{H}}_{n,j}^k$ 'wider' (more columns) than $\mathbf{H}_{n,j}^k$, and that coordination on the receiver side makes $\widetilde{\mathbf{H}}_{n,j}^k$ 'taller' (more rows) than $\mathbf{H}_{n,j}^k$.

B. System model and notation—Asynchronous case

An asynchronous transmission scenario occurs when the DMT blocks of the different users are not aligned in time. We demonstrate this with the example of Fig. 3, where two users (denoted n and j), each with two transceivers, interfere with each other. Their respective DMT blocks are offset by $\beta_{n,j}$, $0 \leq \beta_{n,j} \leq 1$, as shown in the figure. Such a situation gives rise to ICI, which complicates the problem significantly. With ICI, transmission on a given tone k of an interferer influences not only the corresponding tone k of a victim, but all neighboring tones as well.

The bulk of the system model described in Section II continues to be valid for the asynchronous case, including the definition of groups on the transmitter and receiver sides and the fact that more coordination makes the channel matrices increase in size. We assume that all users inside a group either on the transmitter or on the receiver sides are synchronized.

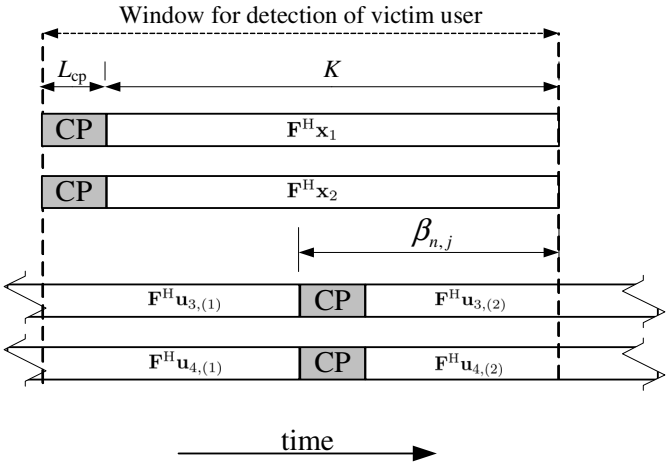

Fig. 3. Model for asynchronous transmission. In this example, two users, each with two transceivers, interfere with one another. Here the victim user, denoted n, has a DMT block for its ith transceiver given by $\mathbf{x}_i$, while the DMT block of the interfering user, denoted j, is denoted by $\mathbf{u}_i$. Symbols from two time instants of the interfering user affect the victim. These instants are denoted by the subscripts (1) and (2). The offset on reception is given by $\beta_{n,j}$, as defined in the figure.

The estimated signal vector for user n on tone k is given by

$$\hat{\mathbf{x}}_n^k = \mathbf{R}_n^k \widetilde{\mathbf{H}}_{n,n}^k \mathbf{T}_n^k \mathbf{x}_n^k + \mathbf{R}_n^k \sum_{\substack{j\in\mathcal{N}\\ j\neq n}} \sum_{s\in\mathcal{K}} \mathbf{A}_{n,j}^{k,s} \mathbf{T}_j^s \mathbf{x}_j^s + \mathbf{B}_{n,j}^{k,s} \mathbf{T}_j^s \bar{\mathbf{x}}_j^s + \mathbf{R}_n^k \mathbf{z}_{\mathcal{G}_q^{\mathrm{rx}}}^k, \quad n \in \mathcal{G}_q^{\mathrm{rx}}. \tag{13}$$

Here $\mathbf{x}_j^s$, $\bar{\mathbf{x}}_j^s$ are the DMT symbols of user j on tone s that interfere with the reception of the DMT symbol of user n on tone k. Symbol $\bar{\mathbf{x}}_j^s$ comes before (in time) the reception of user n and symbol $\mathbf{x}_j^s$ comes after. The matrices $\mathbf{A}_{n,j}^{k,s}$, $\mathbf{B}_{n,j}^{k,s} \in \mathbb{C}^{A_{\mathcal{G}_q^{\mathrm{rx}}} \times A_{\mathcal{G}_i^{\mathrm{tx}}}}$, where q and i are such that $n \in \mathcal{G}_q^{\mathrm{rx}}$ and $j \in \mathcal{G}_i^{\mathrm{tx}}$, account for the ICI. They represent the channel matrices from user j to user n, $j \neq n$, and from tone s to tone k. If $\beta_{n,j} = 0$ or $\beta_{n,j} = 1$, then users n and j are synchronized and there is no ICI. Hence the model in (13) is a generalization of the one in (3). If $\beta_{n,j} = 1$, then $\mathbf{A}_{n,j}^{k,k} = \widetilde{\mathbf{H}}_{n,j}^k$, $\mathbf{A}_{n,j}^{k,s} = \mathbf{0}$ for $k \neq s$ and $\mathbf{B}_{n,j}^{k,s} = \mathbf{0}$ for all s, k. If $\beta_{n,j} = 0$, then $\mathbf{B}_{n,j}^{k,k} = \widetilde{\mathbf{H}}_{n,j}^k$, $\mathbf{B}_{n,j}^{k,s} = \mathbf{0}$ for $k \neq s$ and $\mathbf{A}_{n,j}^{k,s} = \mathbf{0}$ for all s, k. If users n and j belong to the same group in either the receiver or the transmitters sides, then we set $\beta_{n,j} = 0$.

The accurate calculation of the ICI matrices is a fundamental part of the problem. Inaccurate characterizations lead to inaccurate parameters for the optimization problem, which in turn influences the resource allocation and performance. This characterization was attempted only for the single input, single output (SISO) IC case in [16], [18], [21]. For the general, MIMO case we detail how to accurately calculate the ICI matrices $\mathbf{A}_{n,j}^{k,s}$ and $\mathbf{B}_{n,j}^{k,s}$ as a function of a fixed offset $\beta_{n,j}$ in the Appendix.

In order to show the ICI, we briefly focus on the SISO IC case with two users, where the received signal for say, user 1, is written as

$$y_1^k = h_{1,1}^k x_1^k + \sum_{s\in\mathcal{K}} A_{1,2}^{k,s} x_2^s + B_{1,2}^{k,s} \bar{x}_2^s + z_1^k \tag{14}$$

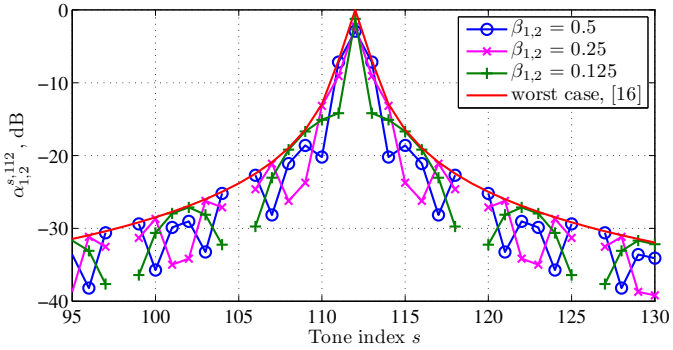

Fig. 4. ICI coefficients $\alpha_{1,2}^{s,112}$ for the SISO IC calculated for different values of $\beta_{1,2}$ as in the Appendix A. We use an ADSL system ($K = 224$) and a frequency flat crosstalk channel. We show only the 35 largest coefficient around tone 112. We also show the worst case coefficients of [16].

Considering $\mathrm{E}\left[(x_n^k)^* x_n^k\right] = \mathrm{E}\left[(\bar{x}_n^k)^* \bar{x}_n^k\right] = p_n^k \ \forall n$, the SNR for user 1 on tone k is given by $p_1^k \left|h_{1,1}^k\right|^2 \left(\sigma_1^k + \sum_{s\in\mathcal{K}} \alpha_{1,2}^{k,s} p_2^s\right)^{-1}$, where we define $\alpha_{1,2}^{k,s} = (A_{1,2}^{k,s})^2 + (B_{1,2}^{k,s})^2$—in contrast to the MIMO case, for the SISO IC case the ICI from tone s to tone k can be characterized with a single scalar. We plot these scalars for an ADSL network with an interfering and a victim user with different offsets in Fig. 4. The crosstalk channel is chosen with impulse response equal to $\mathbf{g}_{1,2} = \begin{bmatrix}1 & 0 & 0 & \dots & 0\end{bmatrix}^{\mathrm{T}} \in \mathbb{C}^L$ (see the Appendix to see how this influences the ICI coefficients). In the figure, we see how the ICI spreads power through frequency as $\beta_{1,2}$ increases. We also show the ICI coefficients calculated in [16], which are calculated considering a worst case situation and are too pessimistic.

Just as in (4), the received signal vector in (13) is processed by the receive matrix $\mathbf{R}_n^k$ for every user and tone. In this paper, we use the linear MMSE (LMMSE) receiver, which is given by

$$\mathbf{R}_n^k = (\mathbf{T}_n^k)^{\mathrm{H}} (\widetilde{\mathbf{H}}_{n,n}^k)^{\mathrm{H}} \left(\mathbf{M}_n^k + \widetilde{\mathbf{H}}_{n,n}^k \mathbf{T}_n^k (\mathbf{T}_n^k)^{\mathrm{H}} (\widetilde{\mathbf{H}}_{n,n}^k)^{\mathrm{H}}\right)^{-1}, \tag{15}$$

where, considering $\mathrm{E}\left[\mathbf{x}_n^s (\mathbf{x}_n^s)^{\mathrm{H}}\right] = \mathrm{E}\left[\bar{\mathbf{x}}_n^s (\bar{\mathbf{x}}_n^s)^{\mathrm{H}}\right] = \mathbf{I}_{A_n} \ \forall n$, the noise covariance matrix $\mathbf{M}_n^k$ is given by

$$\mathbf{M}_n^k = \sum_{\substack{j\in\mathcal{N}\\ j\neq n}} \sum_{s\in\mathcal{K}} \mathbf{A}_{n,j}^{k,s} \mathbf{T}_j^s (\mathbf{T}_j^s)^{\mathrm{H}} (\mathbf{A}_{n,j}^{k,s})^{\mathrm{H}} + \mathbf{B}_{n,j}^{k,s} \mathbf{T}_j^s (\mathbf{T}_j^s)^{\mathrm{H}} (\mathbf{B}_{n,j}^{k,s})^{\mathrm{H}} + \mathbf{I}_{A_{\mathcal{G}_q^{\mathrm{rx}}}}. \tag{16}$$

Although we do not write it explicitly, this matrix can be normalized by a SNR gap Γ. It is well known that the LMMSE receiver is optimal given a set of fixed transmit matrices $\mathbf{T}_n^k$.

The optimization problem we consider is the maximization of the weighted rate sum (WRS) of the participating users in the network subject to per-user power constraints (PC). Consider $\mathcal{T} = \{\mathbf{T}_n^k | n \in \mathcal{N},\ k \in \mathcal{K}\}$. The optimization

TABLE I
COMPARISON OF PREVIOUS SOLUTIONS

Solution [reference]†	Description	Restrictions‡
IWF, OSB, ISB, SCALE, DSB, 2SB, ASB, MIW, NDW-DSM, IPP, MRL-ASB, BPSM [17], [22]–[32]	solutions to SISO spectrum management	$A_n = 1\ \forall n$, IC, synchronous
ZF-GDFE [5]	ZF, (non-linear) GDFE and waterfilling	$A_n = 1\ \forall n$, BC or MAC, synchronous
ZF [7], [8]	linear ZF plus waterfilling	$A_n = 1\ \forall n$; BC or MAC, diagonally dominant channel matrix, synchronous
Low complexity linear ZF [12]	linear ZF, lower complexity version	$A_n = 1\ \forall n$, BC or MAC, diagonally dominant channel matrix, synchronous
MAC-OSB [33]	MMSE-GDFE plus OSB	MAC, $A_n = 1\ \forall n$, synchronous
SVD [9], [10]	SVD applied to channel matrix	MIMO point-to-point, synchronous
Vectoring with common mode [11]	SVD applied to channel matrix of each user, inter-user interference with GDFE	IC, synchronous
IC-MAC OSB/ IC-BC OSB [14], [15]	MMSE-GDFE plus OSB	Partial MAC ($I = N$, $Q < N$, with $\mathcal{G}_n^{\text{tx}} = \{n\},\ n \in \mathcal{N}$ and Q groups on receiver) or partial BC ($I < N$, $Q = N$, with $\mathcal{G}_n^{\text{rx}} = \{n\},\ n \in \mathcal{N}$ and I groups on transmitter), $A_n = 1\ \forall n$, synchronous
WMMSE-GDSB [20]	WMMSE solution for signal coordination plus generalized DSB for power allocation	IC, synchronous
MIW, ASB-A1, ASB-A2, GPS/GPA [16], [17], [28],	solutions to SISO spectrum management, asynchronous case	$A_n = 1\ \forall n$, IC

† A list of the acronyms is given as follows: optimal spectrum balancing (OSB), single input, single output (SISO), generalized decision feedback equalization (GDFE), zero forcing (ZF), minimum mean squared error (MMSE), weighted MMSE (WMMSE) and singular value decomposition (SVD).
‡ In the notation of this paper, a BC is characterized by $I = 1$, $Q = N$, $\mathcal{G}_1^{\text{tx}} = \{1, \ldots, N\}$ and $\mathcal{G}_n^{\text{rx}} = \{n\},\ n \in \mathcal{N}$; a MAC is characterized by $I = N$, $Q = 1$, $\mathcal{G}_n^{\text{tx}} = \{n\},\ n \in \mathcal{N}$ and $\mathcal{G}_1^{\text{rx}} = \{1, \ldots, N\}$; a MIMO point-to-point system is characterized by $I = Q = 1$, $\mathcal{G}_1^{\text{tx}} = \mathcal{G}_1^{\text{rx}} = \{1, \ldots, N\}$; and an IC is characterized by $I = Q = N$ and $\mathcal{G}_n^{\text{tx}} = \mathcal{G}_n^{\text{rx}} = \{n\}, n \in \mathcal{N}$.

problem is then given as

$$\begin{aligned} \max_{\mathcal{T},\mathbf{P}} \quad & \sum_{n\in\mathcal{N}} \sum_{k\in\mathcal{K}} u_n b_n^k \\ \text{subject to} \quad & \text{tr}\{\mathbf{T}_n^k (\mathbf{T}_n^k)^{\text{H}}\} = p_n^k,\ k \in \mathcal{K},\ n \in \mathcal{N} \\ & \sum_{k\in\mathcal{K}} p_n^k \le P_n^{\max},\ n \in \mathcal{N} \end{aligned} \tag{17}$$

Here, with (15) and (16) in hands and assuming Gaussian signaling, we write the data rate for user n and tone k as

$$b_n^k = \log\left|\mathbf{I}_{A_n} + (\mathbf{T}_n^k)^{\text{H}} (\widetilde{\mathbf{H}}_{n,n}^k)^{\text{H}} (\mathbf{M}_n^k)^{-1} \widetilde{\mathbf{H}}_{n,n}^k \mathbf{T}_n^k\right|. \tag{18}$$

Here $\log(\cdot)$ denotes the natural logarithm. The total data rate of user n in bits per second is given by $r_n = {f_s}/{\log(2)} \sum_{k\in\mathcal{K}} b_n^k$, where f_s is the symbol rate. Throughout this paper, we ignore the practical constraint of discrete bit loading.

Still in (17), the variables u_n are weights or priorities given to each user and $P_n^{\max}$ is the PC for user n. We remark that in [34] a similar problem is treated with per-transceiver PCs, whereas here a per-user PC is considered. The situation with the per-transceiver PCs adds complexity to the problem, and for simplicity is not considered in this paper.

The optimization problem in (17) is NP-hard [35], which makes it very challenging. The challenge is twofold. On the one hand, the transmit matrices, i.e. $\mathcal{T}$, should be designed so that the desired signal is easy to identify and the undesired signals are easy to cancel. On the other hand, power should be carefully allocated for every user and tone depending on the signal to noise ratio. These two challenges have a strong interplay with each other. The choice of $\mathcal{T}$ determines the spatial separation or spatial multiplexing that is characteristic of MIMO systems. How this separation occurs depends on the kind of coordination present on both sides of the network. Notice that more transmitter and receiver coordination makes the channel matrices 'wider' or 'taller', which means that there are more dimensions in which this separation can take place. For a (synchronous) MIMO point-to-point system, perfect spatial separation is possible. In this particular case, the singular value decomposition (SVD) of the channel matrix separates the channel in independent eigenmodes, one for each data stream (e.g. [36], [37]). For anything with less coordination, there will be some residual interference that every user has to withstand. Users should avoid excessive residual interference to each other by choosing a smart power allocation through frequency, i.e. by choosing $\mathbf{P}$.

Table I reviews previous solutions this the problem. We give preference to papers dealing with DSL. As we already mentioned, all previous work focuses on special assumptions on the network infrastructure. The majority focuses solely on the synchronous case. As we briefly describe the previous solutions in Table I, we always use the framework just discussed.

III. PROPOSED SOLUTION

In [20], a solution for the synchronous DMT MIMO IC is proposed that achieves good results and is polynomial time solvable. The problem is divided in signal and spectrum coordination parts and these two parts are solved iteratively and independently. The algorithm in [20] is of special interest here, because it forms the basis of the general algorithm that is presented in this paper.

The solution of [20] begins with an equation of the estimated signal vector similar to (12). The difference is that for the general, possibly asynchronous case with any kind of groupings on both sides of the network we use the channel matrices $\mathbf{A}_{n,j}^{k,s}$ and $\mathbf{B}_{n,j}^{k,s}$, whereas in [20] there is a restriction that $\mathbf{A}_{n,j}^{k,k} = \mathbf{H}_{n,j}^{k}\ \forall n,j,k$, $\mathbf{A}_{n,j}^{k,s} = \mathbf{0}\ \forall n,j,k \neq s$ and $\mathbf{B}_{n,j}^{k,s} = \mathbf{0}\ \forall n,j,k,s$. The main insight of this paper is that independently of what channel matrix is used, the solution of [20] still applies. In the following, we derive the main parts of the algorithm while emphasizing the main differences between the current problem and that of [20].

We begin by writing the Lagrangian of (17) as

$$L(\mathcal{T},\mathbf{P},\boldsymbol{\mu},\boldsymbol{\lambda}) = \sum_{n\in\mathcal{N}}\sum_{k\in\mathcal{K}} u_n b_n^k - \sum_{n\in\mathcal{N}} \lambda_n\big(\sum_{k\in\mathcal{K}} p_n^k - P_n^{\max}\big) - \sum_{n\in\mathcal{N}}\sum_{k\in\mathcal{K}} \mu_n^k\big(\mathrm{tr}\big\{\mathbf{T}_n^k(\mathbf{T}_n^k)^{\mathrm{H}}\big\} - p_n^k\big) \tag{19}$$

Here $\boldsymbol{\lambda} = \begin{bmatrix}\lambda_1 & \dots & \lambda_N\end{bmatrix}^{\mathrm{T}} \in \mathbb{R}_+^N$ and $\boldsymbol{\mu} = \begin{bmatrix}\mu_1^1 & \dots & \mu_1^k & \mu_2^1 & \dots & \mu_N^K\end{bmatrix}^{\mathrm{T}} \in \mathbb{R}^{NK}$ are Lagrange multipliers associated respectively with the per-user PCs and the per-user and per-tone trace constraint on the transmit matrices.

In our approach, we separate the problem in two parts. First, we solve for the transmit matrices while keeping the power allocation matrix fixed, then we solve for the power allocation matrix while keeping the transmit matrices fixed. Towards this end, we write (19) as a function of $\mathcal{T}$ and $\boldsymbol{\mu}$; and $\mathbf{P}$ and $\boldsymbol{\lambda}$, respectively as

$$L(\mathcal{T},\boldsymbol{\mu}) = \sum_{n\in\mathcal{N}}\sum_{k\in\mathcal{K}} u_n b_n^k - \sum_{n\in\mathcal{N}}\sum_{k\in\mathcal{K}} \mu_n^k\big(\mathrm{tr}\big\{\mathbf{T}_n^k(\mathbf{T}_n^k)^{\mathrm{H}}\big\} - p_n^k\big) \tag{20}$$

$$L(\mathbf{P},\boldsymbol{\lambda}) = \sum_{n\in\mathcal{N}}\sum_{k\in\mathcal{K}} u_n b_n^k - \sum_{n\in\mathcal{N}} \lambda_n\big(\sum_{k\in\mathcal{K}} p_n^k - P_n^{\max}\big) \tag{21}$$

For the following derivation, we decompose the transmit matrices as $\mathbf{T}_n^k = \sqrt{p_n^k}\overline{\mathbf{T}}_n^k$, where $\mathrm{tr}\big\{\overline{\mathbf{T}}_n^k(\overline{\mathbf{T}}_n^k)^{\mathrm{H}}\big\} = 1$. While solving for $\mathbf{P}$ we keep $\overline{\mathbf{T}}_n^k$ for all n and k fixed and while solving for $\mathcal{T}$ we keep $\mathbf{P}$ fixed.

The important thing to notice about (20) is that now each tone has its PC fixed for all the users, which simplifies the problem significantly. However, unlike the synchronous situation discussed in [20], the problem cannot be solved for each tone separately. The asynchronous transmission couples the optimization through the tones.

The important thing about (21) is that it is a pure power allocation problem, just like [22], [23], [25]–[27], [29]. It is, however, a MIMO power allocation problem, whereas all the references just cited treat a SISO situation. The problem in $\mathbf{P}$ is coupled through frequency by the PCs.

A. Solving for $\mathcal{T}$

To solve (20), we follow the weighted MMSE (WMMSE) approach [20], [38], [39]. This approach establishes a way to maximize rate by minimizing the weighted mean squared error (MSE) of symbol detection. To use this method, for all users and tones we first calculate (15) and calculate a weighting matrix $\mathbf{W}_n^k \in \mathbb{C}^{A_n\times A_n}$ as

$$\mathbf{W}_n^k = u_n(\mathbf{E}_n^k)^{-1} \tag{22}$$

Here

$$\mathbf{E}_n^k = \big((\mathbf{T}_n^k)^{\mathrm{H}}(\widetilde{\mathbf{H}}_{n,n}^k)^{\mathrm{H}}(\mathbf{M}_n^k)^{-1}\widetilde{\mathbf{H}}_{n,n}^k\mathbf{T}_n^k + \mathbf{I}_{A_n}\big)^{-1} \tag{23}$$

is the MSE matrix of symbol detection. The weighting matrix $\mathbf{W}_n^k$ is the key to making the connection between the WRS maximization and the weighted MSE minimization [20], [38], [39].

To solve for $\mathbf{T}_n^k$ we formulate the weighted MMSE minimization problem subject to per-user and per-tone PCs. If the weighting matrix is calculated with (22), then a stationary point of the weighted MSE minimization problem is also a stationary point of the WRS maximization problem. We solve the former because it is a convex problem. The solution for $\mathbf{T}_n^k$ is given by (25), on the top of the next page. Here, the Lagrange multiplier μ_n^k should be chosen such that the PC is respected.

The main difference between (22) and (25) and the equivalent equations in [20] is that the channel matrices $\mathbf{A}_{n,j}^{k,s}$ and $\mathbf{B}_{n,j}^{k,s}$ replace the MIMO IC matrices $\mathbf{H}_{n,j}^k$. Notice that these matrices take into account both any grouping on the transmitter and receiver sides and the possibility of asynchronous transmission. Because of the extra dimensions offered by coordination of different users on the transmitter side, transmit matrices $\mathbf{T}_n^k$ are larger or at least as large as the ones in [20].

B. Solving for $\mathbf{P}$

To solve for $\mathbf{P}$, we take a per-user approach, i.e. we solve for each user separately while keeping power for all other users fixed. To solve for user n in (21), we first notice that $L(\mathbf{p}_n,\lambda_n)$ has a difference of convex (DC) programming structure, i.e. it is the difference of convex functions in p_n^k: while b_n^k is concave in p_n^k, b_j^s, $j\neq n$, is convex.[4] To more easily solve the problem, we first approximate b_j^s, $j\neq n$, by its first order Taylor expansion. With these approximations, we write

$$\tilde{L}(\mathbf{p}_n,\lambda_n) = \sum_{k\in\mathcal{K}} u_n b_n^k + \sum_{\substack{j\in\mathcal{N}\\ j\neq n}}\sum_{s\in\mathcal{K}} u_j\Big(b_j^s\Big|_{\bar{\mathbf{P}}} + (p_n^k - \bar{p}_n^k)\frac{\partial b_j^s}{\partial p_n^k}\Big|_{\bar{\mathbf{P}}}\Big) - \lambda_n p_n^k, \tag{27}$$

which is now concave in p_n^k. Here $\bar{\mathbf{P}}$ and $\bar{p}_n^k$ represent values from a previous iteration. To solve this concave problem, we take the derivative in p_n^k and set it to zero. We obtain

$$\frac{\partial\tilde{L}(\mathbf{p}_n,\lambda_n)}{\partial p_n^k} = u_n\mathrm{tr}\Big\{\Big(p_n^k\mathbf{S}_n^k + \mathbf{I}_{A_n}\Big)^{-1}\mathbf{S}_n^k\Big\} - \lambda_n - \tau_n^k = 0, \tag{28}$$

where $\mathbf{S}_n^k = (\overline{\mathbf{T}}_n^k)^{\mathrm{H}}(\widetilde{\mathbf{H}}_{n,n}^k)^{\mathrm{H}}(\mathbf{M}_n^k)^{-1}\widetilde{\mathbf{H}}_{n,n}^k\overline{\mathbf{T}}_n^k$ and τ_n^k is given by (26), on the top of the next page. In (26), $\mathbf{E}_j^k$ is given by (23).

It may not look like so at first sight, but (28) is a kind of waterfilling equation. Eq. (28) is a generalization of the classical

[4]There is one exception to this, namely the case of the MAC with equal weights for all users. See e.g. [40]

$$\mathbf{T}_n^k = \Big((\widetilde{\mathbf{H}}_{n,n}^k)^{\mathrm{H}}(\mathbf{R}_n^k)^{\mathrm{H}}\mathbf{W}_n^k\mathbf{R}_n^k\widetilde{\mathbf{H}}_{n,n}^k + \sum_{\substack{j\in\mathcal{N}\\ j\neq n}}\sum_{s\in\mathcal{K}}(\mathbf{A}_{j,n}^{s,k})^{\mathrm{H}}(\mathbf{R}_j^s)^{\mathrm{H}}\mathbf{W}_j^s\mathbf{R}_j^s\mathbf{A}_{j,n}^{s,k}+ (\mathbf{B}_{j,n}^{s,k})^{\mathrm{H}}(\mathbf{R}_j^s)^{\mathrm{H}}\mathbf{W}_j^s\mathbf{R}_j^s\mathbf{B}_{j,n}^{s,k} + \mu_n^k\mathbf{I}_{A_{\mathcal{G}_i^{\mathrm{tx}}}}\Big)^{-1} \times (\widetilde{\mathbf{H}}_{n,n}^k)^{\mathrm{H}}(\mathbf{R}_n^k)^{\mathrm{H}}\mathbf{W}_n^k,\ n\in\mathcal{G}_i^{\mathrm{tx}} \quad (25)$$

$$\tau_n^k \triangleq \sum_{\substack{j\in\mathcal{N}\\ j\neq n}}\sum_{s\in\mathcal{K}}\frac{u_j\partial b_j^s}{\partial p_n^k} = \sum_{\substack{j\in\mathcal{N}\\ j\neq n}}\sum_{s\in\mathcal{K}} u_j\mathrm{tr}\Big\{\mathbf{E}_j^s(\mathbf{T}_j^s)^{\mathrm{H}}(\widetilde{\mathbf{H}}_{j,j}^s)^{\mathrm{H}}(\mathbf{M}_j^s)^{-1}\Big(\mathbf{A}_{j,n}^{s,k}\overline{\mathbf{T}}_n^k(\overline{\mathbf{T}}_n^k)^{\mathrm{H}}(\mathbf{A}_{j,n}^{s,k})^{\mathrm{H}} + \mathbf{B}_{j,n}^{s,k}\overline{\mathbf{T}}_n^k(\overline{\mathbf{T}}_n^k)^{\mathrm{H}}(\mathbf{B}_{j,n}^{s,k})^{\mathrm{H}}\Big) \times (\mathbf{M}_j^s)^{-1}\widetilde{\mathbf{H}}_{j,j}^s\mathbf{T}_j^s\Big\} \quad (26)$$

waterfilling in several directions: whereas the classical formula considers a single user synchronous SISO transmission, (28) works for a multi-user (possibly) asynchronous MIMO transmission with any kind of coordination on the transmitter and the receiver sides.[5] In (28), τ_n^k works by distorting the water level so that tones of user n that cause excessive interference to other users and tones are punished and hence are allocated less power. The water level is thus not constant, but frequency selective.

It can be shown that (28) has at most one nonnegative root and that this equation can be simplified to a polynomial form [20]. For solving it, we need but to solve the polynomial and pick the largest root.

The polynomial is of degree A_n. When A_n is large, it may be too costly to solve the polynomial and pick the largest root. Since $A_n - 1$ roots should be discarded anyway, in [20] the power method has been proposed to obtain the largest root of the polynomial. Here we exploit the fact that (28) is the derivative of a concave function, and thus it can have only one zero. To find its zero, we can use e.g. the Newton method.

GF-WMMSE-GDSB

1 Initialize $\mathbf{T}_n^k \forall n,k$ and $\mathbf{P}$;
2 **repeat**
3 Calculate τ_n^k with (26) $\forall n,k$;
4 Calculate $\mathbf{S}_n^k \triangleq (\overline{\mathbf{T}}_n^k)^{\mathrm{H}}(\widetilde{\mathbf{H}}_{n,n}^k)^{\mathrm{H}}(\mathbf{M}_n^k)^{-1}\widetilde{\mathbf{H}}_{n,n}^k\overline{\mathbf{T}}_n^k\ \forall n,k$;
5 **for** $n = 1,\ldots,N$ **do**
6 **repeat**
7 Solve (28) to obtain p_n^k;
8 **if** $\sum_k p_n^k > P_n^{\max}$ **then**
9 increase λ_n;
10 **else**
11 decrease λ_n;
12 **until** $\lambda_n\big|\sum_k p_n^k - P_n^{\max}\big| < \epsilon$
13 Calculate $\mathbf{R}_n^k$ with (15) $\forall n,k$;
14 Calculate $\mathbf{W}_n^k$ with (22) $\forall n,k$;
15 **for** $n = 1,\ldots,N$ **do**
16 **for** $k = 1,\ldots,K$ **do**
17 **repeat**
18 Calculate $\mathbf{T}_n^k$ with (25);
19 **if** $\mathrm{tr}\{\mathbf{T}_n^k(\mathbf{T}_n^k)^{\mathrm{H}}\} > p_n^k$ **then**
20 increase μ_n^k;
21 **else**
22 decrease μ_n^k;
23 **until** $\big|\mathrm{tr}\{\mathbf{T}_n^k(\mathbf{T}_n^k)^{\mathrm{H}}\} - p_n^k\big| < \epsilon$
24 **until** *convergence*

C. Algorithm

We are now ready to write a general algorithm that applies to any number of users, to any number of transceivers, to any number of tones, to any kind of coordination on both the transmitter and on the receiver sides, and to synchronous/asynchronous transmission. Because of the general framework containing the BC, MAC, IC or any combination of them, the WMMSE approach to solve the signal coordination problem and the generalized DSB [20], [26] approach to solve the spectrum coordination part, we call it general framework WMMSE-GDSB (GF-WMMSE-GDSB).

In the algorithm, we first solve for the power matrix and then for the transmit matrices. In lines 3 and 4 we calculate the per-tone penalties and the $\mathbf{S}_n^k$ matrix for all tones and users. The interference plus noise covariance matrix is given by (16).

In line 7 we solve for p_n^k for a given Lagrange multiplier. As mentioned in [20] and also earlier in this paper, this can be done by solving a polynomial and picking the largest root. Other possibilities include using the power method or the Newton method. The next step in the algorithm is to adjust the Lagrange multiplier so that the PCs are satisfied.

The next step is to solve for the matrices $\mathbf{T}_n^k$ for fixed $\mathbf{P}$. As mentioned before, this implies solving K problems with fixed PCs, one for each tone. We solve first for $\mathbf{R}_n^k$ and for $\mathbf{W}_n^k$ in lines 13-14. The loop that follows calculates $\mathbf{T}_n^k$ with (25) and finds the appropriate Lagrange multiplier. We remark that when solving for $\mathbf{T}_n^k$, we are solving a problem with an equality constraint given by $\mathrm{tr}\{\mathbf{T}_n^k(\mathbf{T}_n^k)^{\mathrm{H}}\} = p_n^k$. This means that the Lagrange multipliers μ_n^k can be negative.

The computational complexity of the proposed algorithm is estimated as follows: The computational complexity of the spectrum coordination part is dominated by the calculation of τ_n^k. For each user, the calculation of τ_n^k for one user entails complexity of the order $K^2N(A_n)^3$, where the term $(A_n)^3$ is due to matrix inversions and multiplications. This should be repeated for all users, which implies a complexity of $O(K^2N^2\max_n((A_n)^3))$. For the special case of synchronous transmission, this is reduced to $O(KN^2\max_n((A_n)^3))$. Computational complexity of the signal coordination part is dominated by the calculation of $\mathbf{T}_n^k$. For one user, calculation of this matrix entails complexity of the order of $K^2N(A_n)^3$. This

[5] If we are considering the SISO case, (28) assumes a more familiar form, where power allocation for a given user and tone is given by the water level minus the noise to channel ratio.

should be repeated for all users, which implies a complexity of $O(K^2N^2\max_n((A_n)^3))$. For the special case of synchronous transmission this is reduced to $O(KN^2\max_n((A_n)^3))$.

The algorithm has been extensively experimented with and has always been observed to produce a monotonically increasing objective function. Hence it has always been observed to converge. Because we are explicitly solving the stationary conditions of the problem, at convergence we reach at least a local optimum of the problem.

We remark that the GF-WMMSE-GDSB generalizes some established previously proposed algorithms, most of them being well-known in the field and some of them with proved convergence. For the synchronous DMT SISO IC case, the proposed algorithm is equivalent to the DSB [26]. For the asynchronous DMT SISO IC case, it boils down to the MIW [28]. For synchronous DMT MIMO IC, it is equivalent to the algorithm in [20]. For the MIMO IC and MIMO BC, it is equivalent to the algorithms in [38], [39].

We also remark that the DMT-WMMSE algorithm proposed in [20] could be eventually used for the same purpose of the GF-WMMSE-GDSB. The difference between these two algorithms is that, in the former, signal and spectrum coordination are done jointly, while for the later the two types of coordination are done iteratively. Although the two algorithms have similar performance, in this paper we opt for the GF-WMMSE-GDSB for two reasons. First, it is observed from experiments that the GF-WMMSE-GDSB converges in a significantly smaller number of iterations, which leads in most scenarios to lower time complexity (see e.g. [20]). Second, the spectrum coordination part of the algorithm (i.e. the GDSB part) can be used with any signal coordination algorithm. We do not necessarily need to combine it with a WMMSE type algorithm. We could eventually combine it with e.g. an interference alignment algorithm. This gives us some flexibility.

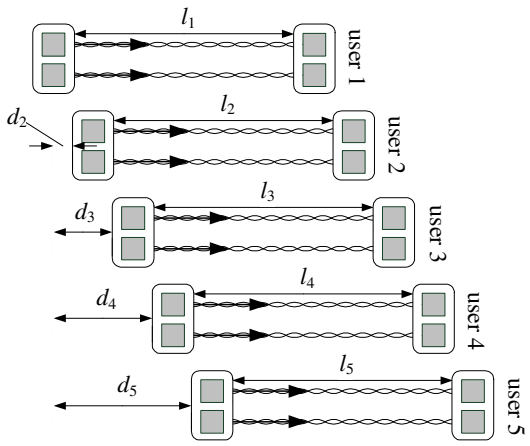

Fig. 5. Downstream ADSL scenario.

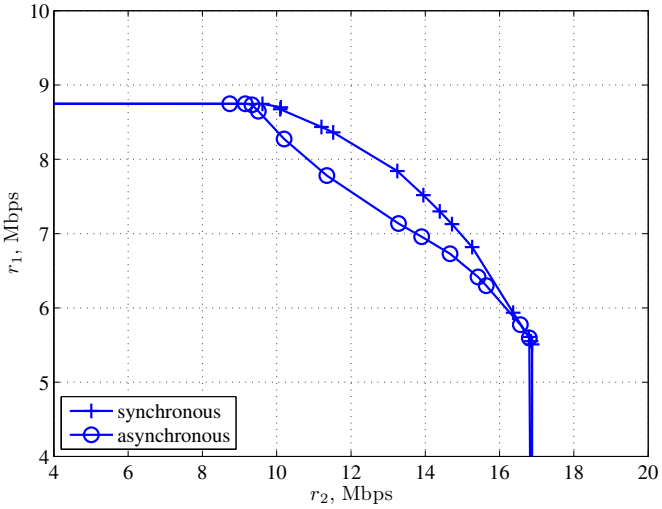

Fig. 6. Rate region for the downstream ADSL scenario with two active users. Referring to Fig. 5, we use $\mathbf{l} = [4\ \ 3]^{\mathrm{T}}$ km and $\mathbf{d} = [0\ \ 3]^{\mathrm{T}}$ km.

IV. Simulation Results

A. Downstream ADSL

The first of our simulation scenarios is the ADSL downstream near-far scenario shown in Fig. 5. There are in total five users, each with two transceivers (two direct modes), i.e. $A_n = 2\ \forall n$. Referring to the figure, we define the line lengths in the vector $\mathbf{l} = [l_1 \quad \dots l_5]^{\mathrm{T}}$. We similarly define $\mathbf{d} = [d_1 \ \dots \ d_5]^{\mathrm{T}}$. The channel gains are calculated according to the model of [41]. The system has cables of 0.5 mm (AWG 24) and an SNR gap of 12.8 dB. Carrier spacing is given by $\Delta_f = 4.3125$ kHz and the symbol rate is 4 KHz. Each user has a PC of 23.4 dBm. For each line, noise model ANSI A is adopted.

Our aim is to assess the impact of asynchronous transmission in the performance of our algorithm. Towards this end, we do three experiments with this scenario. In the three of them we simulate a MIMO IC, i.e. $\mathcal{G}_n^{\mathrm{tx}} = \mathcal{G}_n^{\mathrm{rx}} = \{n\},\ n = 1, \dots, 5$ with both synchronous and asynchronous transmission.

In the first experiment, we keep only users 1 and 2 active. We use an offset $\beta_{1,2} = \beta_{2,1} = 0.5$. We set $\mathbf{l} = [4\ \ 3]^{\mathrm{T}}$ km and $\mathbf{d} = [0\ \ 3]^{\mathrm{T}}$ km. In this scenario the user with the short lines has to avoid excessive interference to the user with the long lines. By changing the values of the user weights w_n, we find the two rate regions for the synchronous and asynchronous cases with the GF-WMMSE-GDSB. They can be seen in Fig. 6. We notice that the asynchronous transmission incurs a rate loss of up to 10 %.

In the second experiment, we want to assess the rate loss incurred by asynchronous transmission as the number of users in the network increases. Referring to Fig. 5, we set $\mathbf{l} = [4\ \ 3.75\ \ 3.5\ \ 3.25\ \ 3]^{\mathrm{T}}$ km and $\mathbf{d} = [0\ \ 2.25\ \ 2.5\ \ 2.75\ \ 3]^{\mathrm{T}}$ km. We simulate the scenario four times, first with users 1 and 2 active, then users 1, 2 and 3 active, etc. We set $w_1 = 0.8$ and set the remaining weights to be of equal values (they sum to 1 at the end)—given that user 1 suffers more from crosstalk, we assign higher preference to it. The result of this experiment is depicted in Fig. 7, where we show the number of active users versus the WRS for the GF-WMMSE-GDSB for both synchronous and asynchronous cases. Not surprisingly, asynchronous transmission takes a greater toll on the capacity of the network as the number of users increases. For example, the difference in WRS between synchronous and asynchronous cases for two active users is 0.2 Mbps. For 5 active users, this value is more than 5 times greater.

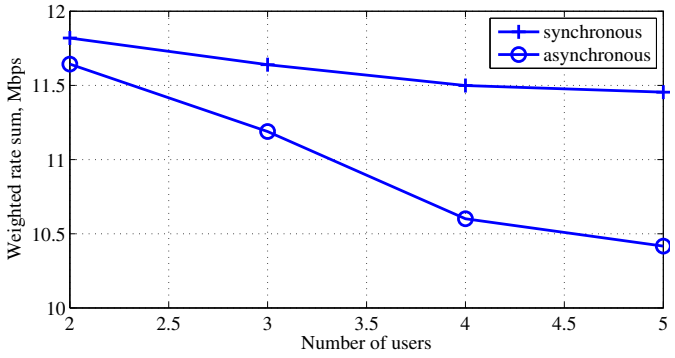

Fig. 7. Weighted rate sum vs. number of active users for the GF-WMMSE-GDSB algorithm for both synchronous and asynchronous cases. Referring to Fig. 5, we set $\mathbf{l} = [4 \quad 3.75 \quad 3.5 \quad 3.25 \quad 3]^{\mathrm{T}}$ km and $\mathbf{d} = [0 \quad 2.25 \quad 2.5 \quad 2.75 \quad 3]^{\mathrm{T}}$ km.

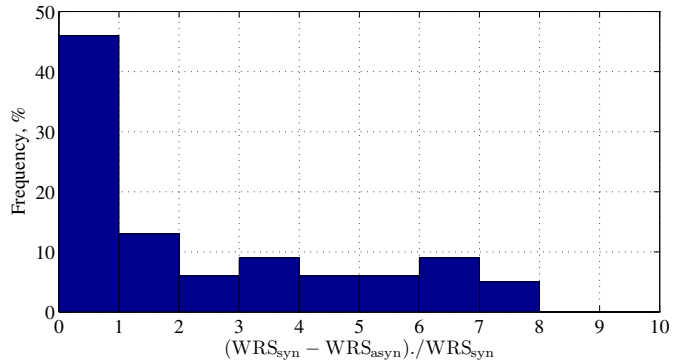

Fig. 8. Histogram for the downstream ADSL scenario with two active users.. Referring to Fig. 5, we set $l_1 = \mathrm{unif}(4, 6)$ km, $l_2 = \mathrm{unif}(4, 6)$ km and $d_2 = \mathrm{unif}(3, l_1)$ km.

In the third experiment, we go back to only two active users. This time we do a Monte-Carlo simulation in order to assess the impact of asynchronous transmission in different instantiation of the network. Referring to Fig. 5, we define $l_1 = \mathrm{unif}(4, 6)$ km, $l_2 = \mathrm{unif}(4, 6)$ km and $d_2 = \mathrm{unif}(3, l_1)$ km. Here we define $\mathrm{unif}(a, b)$ to be a uniformly distributed random variable between a and b. We also set $\beta_{1,2} = \beta_{2,1} = 0.5$. We simulate the GF-WMMSE-GDSB for both synchronous and asynchronous transmission for 100 instantiations of this scenario. For every scenario, we set the user weights as $w_1 = 0.8$ and $w_2 = 0.2$—given that user 1 suffers more from crosstalk, we assign higher preference to it. We plot the histogram of the variable $(\mathrm{WRS}_{\mathrm{syn}} - \mathrm{WRS}_{\mathrm{asyn}})/\mathrm{WRS}_{\mathrm{syn}}$ in Fig. 8. In this simulation we see that the impact of asynchronous transmission can be up to 7 %. Here we see the effectiveness of the GF-WMMSE-GDSB algorithm in the asynchronous case. In 45 % of the cases, there is almost no rate loss in relation to the synchronous case.

B. Upstream G.fast

We simulate the upstream G.fast scenario depicted in Fig. 9. Here, there are 8 users. The 6 users at the top of the figure

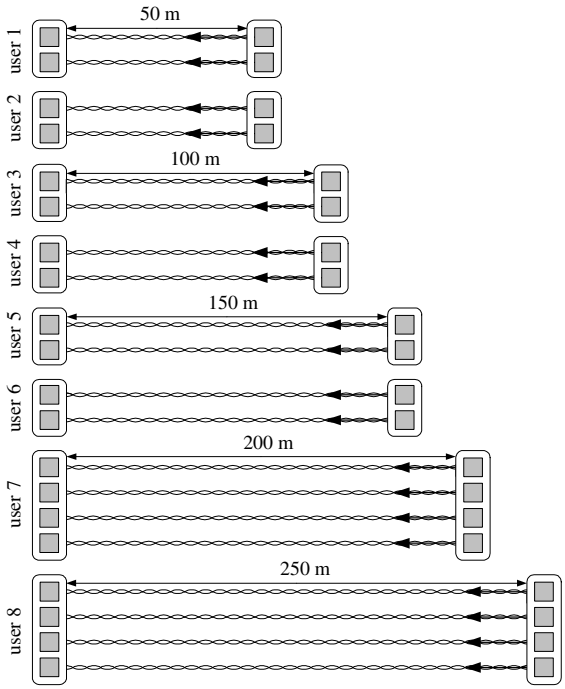

Fig. 9. Upstream G.fast scenario. Here we show the IC scenario.

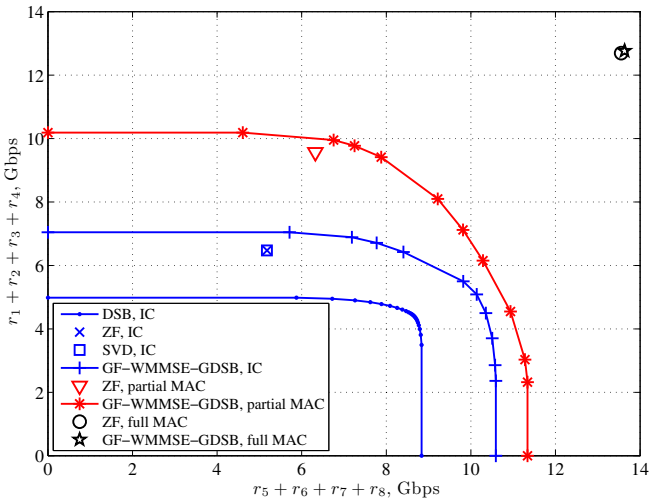

Fig. 10. Rate region for the upstream G.fast scenario.

have each two transceivers, while the two users at the bottom of the figure have each 4 transceivers (all direct modes). We use a maximum power of 4 dBm for each transceiver, which means that the users with two transceivers have a PC of 7 dBm and the users with 4 transceiver have a PC of 10 dBm. The SNR gap is set to 9.45 dB, the carrier spacing is 51.75 KHz and the symbol rate is 48 KHz. The bandwidth of the G.fast standard starts at 2.2 MHz and goes up to 106 MHz—there is a total of $K = 2047$ tones. For this scenario, we use measured channels.

For this experiment, we are interested in assessing the impact of added coordination on the receiver side. There is already some coordination on the transmitter side between the different transceivers of the users. We first simulate an

IC, i.e. the situation when there is only one user in every group on both sides of the network. As mentioned before, this is the situation with the minimum amount of inter-user coordination. We also simulate a *partial MAC*, where there are three groups on the receiver side, as follows: $\mathcal{G}_1^{\mathrm{rx}} = \{1, 2, 3\}$, $\mathcal{G}_2^{\mathrm{rx}} = \{4, 5, 6\}$ and $\mathcal{G}_1^{\mathrm{rx}} = \{7, 8\}$. This grouping could for example indicate that the grouped users belong to the same service provider. Other possibilities would be a sub-loop unbundled scenario, where it is typical to have only a fraction of the end-customers on the signal coordination group or simply that grouped users are all connected to the same box on the CO side of the network. Lastly, we simulate a *full MAC*, i.e. with full receiver coordination. In this case, there is one group on the receiver side, i.e. $\mathcal{G}_1^{\mathrm{rx}} = \{1, \ldots, 8\}$. In Fig. 10, we depict these three respective rate regions. For these rate regions, we always set $w_1 = w_2 = w_3 = w_4$ and $w_5 = w_6 = w_7 = w_8$. By changing the weights, we map the rate regions.

It should come as no surprise that more coordination translates into larger data rates. We remark that signal coordination over all the transceivers provides a substantial improvement compared to partial signal coordination.

In order to be able to assess the performance of our proposal, we also simulate previous solutions. Specifically, we simulate the DSB algorithm [26], the ZF algorithm [7], [8] and the SVD algorithm [9]. We detail the implementation of these solutions in the following paragraphs.

The DSB algorithm is a pure spectrum coordination algorithm. It restricts $\mathbf{R}_n^k$ and $\mathbf{T}_n^k$ to be diagonal. The DSB algorithm does not exploit the intra-user coordination that is possible in this scenario, and it performs poorly.

The ZF algorithm sets $\mathbf{R}_n^k = ((\widetilde{\mathbf{H}}_{n,n}^k)^{\mathrm{H}}\widetilde{\mathbf{H}}_{n,n}^k)^{-1}(\widetilde{\mathbf{H}}_{n,n}^k)^{\mathrm{H}}$ and restricts $\mathbf{T}_n^k$ to be diagonal. To calculate the diagonal elements of $\mathbf{T}_n^k$, it performs power loading on the transmitter side with a waterfilling algorithm. We run the ZF algorithm for the IC, the partial MAC and the full MAC cases. For the IC, inter-user interference is considered Gaussian noise. For the partial MAC case, inter-group interference is considered Gaussian noise. In these cases, the ZF algorithm performs poorly because interference is unaccounted for. For the full MAC case, the ZF algorithm performs almost optimally. Still the use of ZF receivers causes noise enhancement, which translates itself in a slight rate loss in comparison to the GF-WMMSE-GDSB.

The SVD algorithm sets $\mathbf{R}_n^k = (\mathbf{U}_{n,n}^k)^{\mathrm{H}}$ and $\mathbf{T}_n^k = \mathbf{V}_n^k$, where $\mathbf{U}_n^k$ and $\mathbf{V}_n^k$ are respectively the matrices of left and right singular vectors of $\widetilde{\mathbf{H}}_{n,n}^k$. We use this algorithm for the IC case, where inter-user interference is considered Gaussian noise. In this case, the SVD algorithm also performs poorly because inter-user interference is unaccounted for.

V. Conclusion

The resource allocation problem in a multi-user environment has been a popular research topic in the past decade. We notice, however, that the majority of the papers on the subject make strong assumptions about the network infrastructure. E.g., many papers assume that coordination is only available on the service provider side or that all users have only one transceiver. In this paper, we propose a general framework and algorithm for the WRS maximization problem in a multi-user system. Our framework includes systems with any number of users, any number of transceivers, any number of tones, any kind of coordination on both the transmitter and on the receiver sides, and synchronous or asynchronous transmission. In what concerns the coordination, we construct channel matrices from all transmitters to all receivers that have as building blocks the channel matrices relating to the MIMO IC and that depend on the kind of coordination on the transmitter and receiver sides. The algorithm divides the problem into two parts, one dealing with the spectrum coordination (i.e. power allocation) and the other dealing with signal coordination (i.e. the spatial separation typical of MIMO systems).

Some extensions that would be interesting to explore would be per-transceiver PCs and non-linear receivers. Per-transceiver PCs are more realistic than the per-user PCs used in this paper, but they also lead to more complex problems. A solution to this problem is presented for the MIMO IC scenario in [34].

Appendix
Derivation of the ICI matrices

In this appendix we ignore the subscripts denoting users. To evaluate the impact of the asynchronous transmission, we focus on one victim and one interfering user, as depicted in Fig. 3. The victim user, denoted as user 1, has its DMT symbol for its ith transceiver denoted by $\mathbf{x}_i \in \mathbb{C}^K$ (unlike the remainder of this paper the subscript does not denote user). The interfering user, denoted as user 2, has its DMT symbol denoted by $\mathbf{u}_i$. There are a total of $U + V$ transceivers in the network, where U is the number of transceivers for user 1 and V for user 2. We number them sequentially. E.g., if each of the users has two transceivers, we refer to the DMT symbols as $\mathbf{x}_1$, $\mathbf{x}_2$, $\mathbf{u}_3$ and $\mathbf{u}_4$. Symbols $\mathbf{u}_{i,(1)}$ and $\mathbf{u}_{i,(2)}$, $i = U + 1, \ldots, U + V$, interfere with the reception of user 1, where the bracketed subscripts denote time. Without loss of generality, we consider time instants (1) and (2).

Before proceeding, we define some variables. We assume that the CP, whose length is given by L_{cp}, is longer than both the direct and crosstalk channel impulse responses. The offset between the transmission of the two users is given by β, $0 \leq \beta \leq 1$. We define $\mathbf{F}$ and $\mathbf{F}^{\mathrm{H}} \in \mathbb{C}^{K \times K}$ as the DFT and IDFT matrices, respectively. The matrices

$$\widetilde{\mathbf{C}} = \left[\begin{array}{c:c} \mathbf{0}_{K \times L_{\mathrm{cp}}} & \mathbf{I}_K \end{array}\right] \tag{29}$$

and

$$\mathbf{C} = \left[\begin{array}{c:c} \mathbf{0}_{L_{\mathrm{cp}} \times (K - L_{\mathrm{cp}})} & \mathbf{I}_{L_{\mathrm{cp}}} \\ \hdashline \multicolumn{2}{c}{\mathbf{I}_K} \end{array}\right],$$

where $\widetilde{\mathbf{C}} \in \mathbb{R}^{K \times (K + L_{\mathrm{cp}})}$ and $\mathbf{C} \in \mathbb{R}^{(K + L_{\mathrm{cp}}) \times K}$, respectively remove and insert the CP. The matrices $\mathbf{S}_{(1)}$ and $\mathbf{S}_{(2)}$ capture

the effect of the time offset. Define $\omega = \lfloor \beta(K+L_{\rm cp}) \rfloor$ as the number of samples in delay. These matrices are given by

$$\mathbf{S}_{(1)} = \left[\begin{array}{c|c} \mathbf{0}_{(K+L_{\rm cp}-\omega)\times\omega} & \mathbf{I}_{(K+L_{\rm cp}-\omega)} \\ \hline \multicolumn{2}{c}{\mathbf{0}_{\omega\times(K+L_{\rm cp})}} \end{array}\right] \tag{30}$$

and

$$\mathbf{S}_{(2)} = \left[\begin{array}{c} \mathbf{0}_{(K+L_{\rm cp}-\omega)\times(K+L_{\rm cp})} \\ \hline \mathbf{I}_{\omega} \;\; \mathbf{0}_{\omega\times(K+L_{\rm cp}-\omega)} \end{array}\right]. \tag{31}$$

Here $\mathbf{S}_{(1)},\ \mathbf{S}_{(2)} \in \mathbb{R}^{(K+L_{\rm cp})\times(K+L_{\rm cp})}$. If β is equal to zero or one, then the system is synchronized and $\mathbf{S}_{(1)} = \mathbf{I}_{(K+L_{\rm cp})}$ and $\mathbf{S}_{(2)} = \mathbf{0}_{(K+L_{\rm cp})\times(K+L_{\rm cp})}$ or vice-versa.

The signal on the receiver side for user 1 is given by

$$\mathbf{r} = \mathbf{H}\mathbf{x} + \mathbf{A}\mathbf{u}_{(1)} + \mathbf{B}\mathbf{u}_{(2)} + \mathbf{z}. \tag{32}$$

Here $\mathbf{r}, \mathbf{z} \in \mathbb{C}^{UK}$ are respectively the received signal and circularly symmetric zero mean complex Gaussian noise for user 1; the vector $\mathbf{x} = [\mathbf{x}_1^{\rm T} \ldots \mathbf{x}_U^{\rm T}]^{\rm T} \in \mathbb{C}^{UK}$ is the concatenation of the DMT symbols from all transceivers from user 1—the vectors $\mathbf{u}_{(1)}, \mathbf{u}_{(2)} \in \mathbb{C}^{VK}$ are defined similarly; the matrix $\mathbf{H} \in \mathbb{C}^{KU\times KU}$ has a block structure where the (i,s)-th block, $i,s = 1,\ldots,U$, is given by $\mathbf{F}\widetilde{\mathbf{C}}\mathbf{G}_{i,s}\mathbf{C}\mathbf{F}^{\rm H}$; $\mathbf{G}_{i,s} \in \mathbb{C}^{(K+L_{\rm cp})\times(K+L_{\rm cp})}$ is a Toeplitz matrix with first column $\left[\mathbf{g}_{i,s}^{\rm T}\ \mathbf{0}_{1\times(K+L_{\rm cp}-L)}\right]^{\rm T}$ and first row $\left[g_{i,s}(1)\ \mathbf{0}_{1\times(K+L_{\rm cp}-1)}\right]$, where $\mathbf{g}_{i,s} \in \mathbb{C}^L$ is the L-tap channel impulse response from the transmitter of transceiver s to the receiver of transceiver i of user 1 and is considered constant in time; $\mathbf{A}, \mathbf{B} \in \mathbb{C}^{KU\times KV}$ have a block structure, where the $(i, s-U)$-th block, $i = 1,\ldots,U$ and $s = U+1,\ldots,U+V$, are given respectively as $\mathbf{F}\widetilde{\mathbf{C}}\mathbf{G}_{i,s}\mathbf{S}_{(1)}\mathbf{C}\mathbf{F}^{\rm H}$ and $\mathbf{F}\widetilde{\mathbf{C}}\mathbf{G}_{i,s}\mathbf{S}_{(2)}\mathbf{C}\mathbf{F}^{\rm H}$. The matrix $\mathbf{G}_{i,s}$ is, as before, Toeplitz with $\mathbf{g}_{i,s} \in \mathbb{C}^L$ being the L-tap channel impulse response from the transmitter of transceiver s of user two to the receiver of transceiver i of user 1.

Because $L \le L_{\rm cp}$, the process of insertion and removal of the CP creates a square circulant matrix, which is in turn diagonalized by the DFT and IDFT operations. Hence the (i,s)-th block of $\mathbf{H}$, where $i,s = 1,\ldots,U$, is given by $\mathbf{F}\widetilde{\mathbf{C}}\mathbf{G}_{i,s}\mathbf{C}\mathbf{F}^{\rm H} = \mathrm{diag}\{\mathbf{h}_{i,s}\}$, where $\mathbf{h}_{i,s} \in \mathbb{C}^K$ is the corresponding channel frequency response. Because of the offset represented by the matrices $\mathbf{S}_{(1)}$ and $\mathbf{S}_{(2)}$, the operation $\widetilde{\mathbf{C}}\mathbf{G}_{i,s}\mathbf{S}_{(1)}\mathbf{C}$ and $\widetilde{\mathbf{C}}\mathbf{G}_{i,s}\mathbf{S}_{(2)}\mathbf{C}$ fail to produce a circulant matrix, and therein lies the effect of the asynchronicity.

The next step is to write a per-tone version of (32):

$$\mathbf{r}^k = \mathbf{H}^k\mathbf{x}^k + \sum_{s\in\mathcal{K}} \mathbf{A}^{k,s}\mathbf{u}_{(1)}^s + \mathbf{B}^{k,s}\mathbf{u}_{(2)}^s + \mathbf{z}^k. \tag{33}$$

Here $\mathbf{x}^k,\ \mathbf{z}^k \in \mathbb{C}^U,\ \mathbf{u}_{(1)},\ \mathbf{u}_{(2)} \in \mathbb{C}^V$. We define $\mathbf{x}^k = [x_1^k \ \cdots \ x_U^k]^{\rm T}$. Other vectors are defined similarly. We also have $\mathbf{H}^k \in \mathbb{C}^{U\times U}$ and $\mathbf{A}^{k,s}, \mathbf{B}^{k,s} \in \mathbb{C}^{U\times V}$. The matrix $\mathbf{H}^k$ is obtained from $\mathbf{H}$ by substituting the block (i,s) by the (k,k) element of block (i,s), with $i,s = 1,\ldots,U$. The matrices $\mathbf{A}^{k,s},\ \mathbf{B}^{k,s} \in \mathbb{C}^{U\times V}$ are obtained by substituting the block $(i, s-U)$ by the (k,s) element of block $(i, s-U)$, with $i = 1,\ldots,U$ and $s = U+1,\ldots,U+V$.

Substituting $\mathbf{u}_{(1)}^s = \mathbf{T}_u^s\bar{\mathbf{x}}_u^s$ and $\mathbf{u}_{(2)}^s = \mathbf{T}_u^s\mathbf{x}_u^s$, we arrive at (13).

ACKNOWLEDGMENT

The authors wish to thank the anonymous reviewers for several suggestions that have considerably improved the paper.

REFERENCES

[1] H. Bölcskei, D. Gesbert, C. B. Papadias, and A.-J. van der Veen, *Space-Time Wireless Systems: From Array Processing to* MIMO *Communications*. Cambridge University Press, 2006.

[2] D. Gesbert, M. Kountouris, R. W. Heath, Jr., C.-B. Chae, and T. Sälzer, "Shifting the MIMO paradigm," *IEEE Signal Process. Mag.*, vol. 24, no. 5, pp. 36–46, 2007.

[3] J. M. Cioffi, S. Jagannathan, M. Mohseni, and G. Ginis, "CuPON: the copper alternative to PON 100 Gb/s DSL networks," *IEEE Commun. Mag.*, vol. 45, no. 6, pp. 132–139, 2007.

[4] Broadband Forum, "FTTx supercharges broadband deployment," 2013. Available: http://www.broadband-forum.org/news/download/pressreleeases/2013/BBF_FTTx13.pdf

[5] G. Ginis and J. M. Cioffi, "Vectored transmission for digital subscriber line systems," *IEEE J. Sel. Areas Commun.*, vol. 20, no. 5, pp. 1085–1104, 2002.

[6] P. Ödling, T. Magesacher, S. Höst, P. O. Börjesson, M. Berg, and E. Areizaga, "Fourth generation broadband concept," *IEEE Commun. Mag.*, vol. 47, no. 1, pp. 63–69, 2009.

[7] R. Cendrillon, G. Ginis, E. Van den Bogaert, and M. Moonen, "A near-optimal linear crosstalk canceler for upstream VDSL," *IEEE Trans. Signal Process.*, vol. 54, no. 8, pp. 3136–3146, 2006.

[8] ——, "A near-optimal linear crosstalk precoder for downstream VDSL," *IEEE Trans. Commun.*, vol. 55, no. 5, pp. 860–863, 2007.

[9] B. Lee, J. M. Cioffi, S. Jagannathan, and M. Mohseni, "Gigabit DSL," *IEEE Trans. Commun.*, vol. 55, no. 9, pp. 1689–1692, 2007.

[10] V. Le Nir, M. Moonen, J. Verlinden, and M. Guenach, "Full vectoring optimal power allocation in xDSL channels under per-modem power constraints ans spectral mask constraints," *IEEE Trans. Commun.*, vol. 57, no. 1, pp. 194–202, 2009.

[11] S. Jagannathan, V. Pourahmad, J. M. Cioffi, M. Ouzzif, and R. Tarafi, "Common-mode data transmission using the binder sheath in digital subscriber lines," *IEEE Trans. Commun.*, vol. 57, no. 3, pp. 831–840, 2009.

[12] A. Leshem and Y. Li, "A low complexity linear precoding technique for next generation VDSL downstream transmission over copper," *IEEE Trans. Signal Process.*, vol. 55, no. 1, pp. 5527–5534, 2007.

[13] V. Le Nir, M. Moonen, J. Verlinden, and M. Guenach, "Optimal power allocation for downstream xDSL with per-modem total power constraints: broadcast channel optimal spectrum balancing (BC-OSB)," *IEEE Trans. Signal Process.*, vol. 57, no. 2, pp. 690–697, 2009.

[14] A. R. Forouzan, M. Moonen, J. Maes, and M. Guenach, "Joint level 2 and 3 dynamic spectrum management for downstream VDSL," *IEEE Trans. Commun.*, vol. 60, no. 10, pp. 3111–3122, 2012.

[15] ——, "Joint level 2 and 3 dynamic spectrum management for upstream VDSL," *IEEE Trans. Commun.*, vol. 59, no. 10, pp. 2851–2861, 2011.

[16] V. M. K. Chan and W. Yu, "Multiuser spectrum optimization for discrete multitone systems with asynchronous crosstalk," *IEEE Trans. Signal Process.*, vol. 55, no. 11, pp. 5425–5435, 2007.

[17] R. Cendrillon, J. Huang, M. Chiang, and M. Moonen, "Autonomous spectrum balancing for digital subscriber lines," *IEEE Trans. Signal Process.*, vol. 55, no. 8, pp. 4241–4257, 2007.

[18] M. Park, K. Ko, B. Park, and D. Hong, "Effects of asynchronous MAI on average SEP performance of OFDMA uplink systems over frequency-selective Rayleigh fading channels," *IEEE Trans. Commun.*, vol. 58, no. 2, pp. 586–599, 2010.

[19] R. B. Moraes, P. Tsiaflakis, and M. Moonen, "Intercarrier interference in DSL networks due to asynchronous DMT transmission," in *2013 IEEE Int. Conf. Acoust., Speech and Signal Process.*

[20] R. B. Moraes, P. Tsiaflakis, J. Maes, and M. Moonen, "DMT MIMO IC rate maximization in DSL with combined signal and spectrum coordination," *IEEE Trans. Signal Process.*, vol. 61, no. 7, pp. 1756–1769, 2013.

[21] M. Park, K. Ko, H. Yoo, and D. Hong, "Performance analysis of OFDMA uplink systems with symbol timing misalignment," *IEEE Trans. Commun.*, vol. 7, no. 8, pp. 376–378, 2003.
[22] W. Yu, G. Ginis, and J. M. Cioffi, "Distributed multiuser power control for digital subscriber lines," *IEEE J. Sel. Areas Commun.*, vol. 20, no. 5, pp. 1105–1115, 2002.
[23] R. Cendrillon, W. Yu, M. Moonen, J. Verlinden, and T. Bostoen, "Optimal multiuser spectrum balancing for digital subscriber lines," *IEEE Trans. Commun.*, vol. 54, no. 5, pp. 922–933, 2006.
[24] R. Cendrillon and M. Moonen, "Iterative spectrum management for digital subscriber lines," in *2005 IEEE Int. Conf. Commun.*
[25] J. Papandriopoulos and J. S. Evans, "SCALE: a low-complexity distributed protocol for spectrum balancing in multiuser DSL networks," *IEEE Trans. Inf. Theory*, vol. 55, no. 8, pp. 3711–3724, 2009.
[26] P. Tsiaflakis, M. Diehl, and M. Moonen, "Distributed spectrum management algorithms for multiuser DSL networks," *IEEE Trans. Signal Process.*, vol. 56, no. 10, pp. 4825–4843, 2008.
[27] R. B. Moraes, B. Dortschy, A. Klautau, and J. Rius i Riu, "Semiblind spectrum balancing for DSL," *IEEE Trans. Signal Process.*, vol. 58, no. 7, pp. 3717–3727, 2010.
[28] W. Yu, "Multiuser water-filling in the presence of crosstalk," in *2007 Inf. Theory and Appl. Workshop.*
[29] M. Wolkerstorfer, J. Jaldén, and T. Nordström, "Column generation for discrete-rate multi-user and multi-carrier power control," *IEEE Trans. Commun.*, vol. 60, no. 9, pp. 2712–2722, 2012.
[30] Y. Noam and A. Leshem, "Iterative power pricing for distributed spectrum coordination in DSL," *IEEE Trans. Commun.*, vol. 57, no. 4, pp. 948–953, 2009.
[31] S. Huberman, C. Leung, and T. Le-Ngoc, "Constant offset autonomous spectrum balancing using multiple reference lines for VDSL," *IEEE Trans. Signal Process.*, vol. 60, no. 12, pp. 6719–6723, 2012.
[32] W. Lee, Y. Kim, M. Brady, and J. Cioffi, "Band-preference dynamic spectrum management in a DSL environment," in *2006 IEEE Global Telecomm. Conf.*
[33] P. Tsiaflakis, J. Vangorp, J. verlinden, and M. Moonen, "Multiple access channel optimal spectrum balancing for upstream DSL transmission," *IEEE Commun. Lett.*, vol. 11, no. 4, pp. 398–400, 2007.
[34] R. B. Moraes, P. Tsiaflakis, J. Maes, and M. Moonen, "DMT MIMO IC rate maximization in DSL with per-transceiver power constraints," *Signal Process.*, vol. 101, pp. 87–98, 2014.
[35] Z.-Q. Luo and S. Zhang, "Dynamic spectrum management: complexity and duality," *IEEE Trans. Signal Process.*, vol. 2, no. 1, pp. 57–73, 2009.
[36] D. P. Palomar, J. M. Cioffi, and M. A. Lagunas, "Joint tx-rx beamforming design for multicarrier MIMO channels: a unified framework for convex optimization," *IEEE Trans. Signal Process.*, vol. 51, no. 9, pp. 2381–2401, 2003.
[37] I. E. Telatar, "Capacity of multi-antenna Gaussian channels," *European Trans. Telecommun.*, vol. 10, pp. 585–595, 1999.
[38] S. S. Christensen, R. Agarwal, E. de Carvalho, and J. M. Cioffi, "Weighted sum-rate maximization using weighted MMSE for MIMO-BC beamforming design," *IEEE Trans. Wireless Commun.*, vol. 7, no. 12, pp. 4792–4799, 2008.
[39] Q. Shi, M. Razaviyayn, Z.-Q. Luo, and C. He, "An iteratively weighted MMSE approach to distributed sum-utility maximization for a MIMO interfering broadcast channel," *IEEE Trans. Signal Process.*, vol. 59, no. 9, pp. 4331–4340, 2011.
[40] W. Yu, W. Rhee, S. Boyd, and J. M. Cioffi, "Iterative water-filling for Gaussian vector multiple-access channels," *IEEE Trans. Inf. Theory*, vol. 50, no. 1, pp. 145–152, 2004.
[41] ETSI Std. TS 101 270-1, "Transmission and multiplexing (TM); access transmission systems on metallic access cables; very-high bit-rate digital subscriber line transceivers (VDSL); part 1: functional requirements," 2003.



Rodrigo B. Moraes (S'08, M'14) was born in Belém, Brazil, in 1982. He obtained the Bachelor degree at the Federal University of Pará, Belém, Brazil, in 2005, the M.Sc. degree at the Pontifical Catholic University, Rio de Janeiro, Brazil, in 2009, and the Ph.D. degree in 2014 at the KU Leuven, Belgium, all in Electrical Engineering. Since 2014 he is a research engineer at Alcatel-Lucent Bell Labs in Antwerp, Belgium.

Dr. Moraes was a visiting researcher at Ericsson's Broadband Technologies Laboratories, Sweden, in 2006 and at the Telecommunications Research Center Vienna (FTW), Austria, in 2013. His research interests are in signal processing for communications.

Dr. Moraes has received the FAPERJ *Nota Dez* Scholarship by state of Rio de Janeiro, Brazil, the IEEE Travel Grants, and a *best paper award* at the IEEE International Conference on Communications in 2013.



Paschalis Tsiaflakis (S'06, M'09) received the Masters degree in electrical engineering and the Ph.D. degree in engineering sciences from the KU Leuven (Belgium) in 2004 and 2009, respectively, after which he hold a postdoctoral research fellow position from 2010 until 2013. He was a visiting researcher at Princeton University in 2007, a visiting postdoc at the University of California Los Angeles in 2010, and a postdoctoral research associate at the Center for Operations Research and Econometrics in 2011.

He is currently a researcher at Bell Labs Alcatel-Lucent. His research expertise is centered around signal processing and optimization for wireline and wireless communication systems.

Dr. Tsiaflakis received the *Belgian Young ICT Personality* award sponsored by FITCE in 2010, two IEEE ICC best paper awards in 2013, the *Best Multimedia Master Thesis* prize award sponsored by PIMC in 2001, and was a top-12 finalist for the European ERCIM Cor Baayen Award 2010. He also received a FWO Aspirant Grant in 2004, a PDMK postdoc grant in 2009, a Francqui Intercommunity Postdoc Grant in 2010, a FWO postdoc grant in 2011, and a FNRS postdoc grant in 2011.

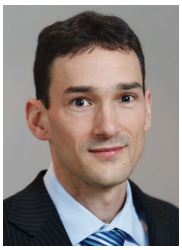

Jochen Maes (M'10, SM'11) joined Alcatel-Lucent Bell Labs in 2006 where he has been continuously shifting the limits of copper. He heads the Bell Labs team that researches transceiver and system design for copper access. The team is currently focused on G.fast that delivers 1 Gb/s over the telephony network. His previous work includes vectoring and phantom mode transmission, which received the Broadband Infovision Award in 2010 and the Bell Labs Presidents Award in 2011. Jochen contributes to ITU G.vector and G.fast projects, is senior member of the IEEE, and holds a Masters degree in Physics and a Ph.D. in Science.



Marc Moonen (M'94, SM'06, F'07) is a Full Professor at the Electrical Engineering Department of KU Leuven, where he is heading a research team working in the area of numerical algorithms and signal processing for digital communications, wireless communications, DSL and audio signal processing.

He received the 1994 KU Leuven Research Council Award, the 1997 Alcatel Bell (Belgium) Award (with Piet Vandaele), the 2004 Alcatel Bell (Belgium) Award (with Raphael Cendrillon), and was a 1997 Laureate of the Belgium Royal Academy of Science. He received a journal best paper award from the IEEE Transactions on Signal Processing (with Geert Leus) and from Elsevier Signal Processing (with Simon Doclo).

He was chairman of the IEEE Benelux Signal Processing Chapter (1998-2002), a member of the IEEE Signal Processing Society Technical Committee on Signal Processing for Communications, and President of EURASIP (European Association for Signal Processing, 2007-2008 and 2011-2012).

He has served as Editor-in-Chief for the *EURASIP Journal on Applied Signal Processing* (2003-2005), and has been a member of the editorial board of IEEE TRANSACTIONS ON CIRCUITS AND SYSTEMS II, *IEEE Signal Processing Magazine*, *Integration-the VLSI Journal*, *EURASIP Journal on Wireless Communications and Networking*, and *Signal Processing*. He is currently a member of the editorial board of *EURASIP Journal on Applied Signal Processing* and Area Editor for Feature Articles in *IEEE Signal Processing Magazine*.